IMPLANTABLE LOOP ANTENNA

by

Maryam Soltan Zadeh

B.Sc., Sharif University of Technology, 2003

A THESIS SUBMITTED IN PARTIAL FULFILLMENT
OF THE REQUIREMENTS FOR THE DEGREE OF
MASTER OF APPLIED SCIENCE
in the School
of
Engineering Science

SIMON FRASER UNIVERSITY
Summer 2006

APPROVAL

Name:	Maryam Soltan Zadeh
Degree:	Master of Applied Science
Title of thesis:	Implantable Loop Antenna
Examining Committee:	Dr. Atousa Hajshirmohammadi, Chair
	Dr. Rodney Vaughan, Senior Supervisor
	Dr. William Dunford, Supervisor
	Dr. Karim Karim, SFU Examiner
Date Approved:	Jun. 27/06.

Abstract

Building a communication link with implanted devices increases capability of diagnosis and treatment and reduces the need for invasive surgical operations. The technology can also be used in tracking animals and gathering their biological information. In this dissertation a loop antenna is proposed for an implanted tag which is to be used under the skin of Steller sea lions for tracking purposes. The impedance of the antenna has been measured inside a tissue simulating liquid. Two types of housings (alumina and ABS) have been used. It has been shown that both housings reduce the effect of surrounding changes on the antenna impedance. Also the impedance of the antenna is not influenced by the changes in the skin tissue thickness. Using the power loss measurements, the range of the antenna is calculated to decrease 40% when implanted. Finally a matching method is proposed to increase the efficiency of the transmission.

To My Beloved, Amir

"We can't solve problems by using the same kind of thinking we used when we created them."

— ALBERT EINSTEIN,*1879-1955*

Acknowledgments

This work was partially funded by UBC Steller sea lion project (Professor Royann Petrell, Professor William Dunford and Professor Andrew Trites), for which I am very grateful.

I would like to express my deepest gratitude to:

- My supervisor Dr. Rodney Vaughan, for all of his support and help throughout this way and for showing me the full meaning of insight in engineering;
- My parents, who gave me the opportunity to start this journey and because of whom I never felt alone;
- My beloved husband Amir for his never ending support and encouragements;
- My friends Laleh, Roozbeh, Sara, Sarah, Shirin and Soroush who made me feel at home;
- All of my great friends around the world;

And finally I want to give my special thanks to my dearest sisters, Nahid and Shahrzad, whose presence gave me the courage and confidence to leave my family.

Contents

List of Tables

List of Figures

Preface

When I began to learn more about implantable antennas, I found out that I would be dealing with a lot of uncertainties throughout the way. I felt that the interactions between the electrical engineering and biological researches need something more than numerical approaches. However most of the available reports on implantable antennas deal with the numerical evaluations of the antenna in fixed numeric models of biological tissues. Instead, in this dissertation, the emphasis has been put on the experimental measurements of the antenna.

One of the main challenges in the way of evaluating the implantable antennas is the sensitivity of the results to the changes in the environment. In this work we study a solution for reducing this sensitivity and isolating the antenna from the changes in surrounding tissues. Consequently the results will be more reliable and the performance of the antenna will meet what is expected to a greater extent. We tried to measure the impedance of the antenna in different environments, in order to design a functional matching circuit for an implantable transceiver.

The power loss issue in the transmission through the biological tissues has also been touched on. A method of matching has been proposed in order to reduce the power loss and improve the efficiency of the communication with implantable antennas.

Parts of this thesis have been presented in:

R. J. Petrell, R. G. Vaughan, R. Virtue, B. Hori, S. Mirabbasi, W. Dunford, A.w. Trites, M. Soltanzadeh, "A Flat Sub-dermal Radio Frequency Identification Tag", in proceedings of the 16th Biennial Conference on the Biology of Marine Mammals, San Diego, California, December 2005.

Chapter 1

Introduction

Medical implantable devices are at the center of much academic and technical research in bioengineering, medicine and biology. The increasing demand for reducing the need for invasive surgical operations necessitates the use of implanted devices as a part of diagnosis and treatment procedure. In recent years, the application of the implantable antenna for building a communication link between the implanted devices and outside the human body is receiving more attention. The possibility of gathering data from an implanted device inside the body of an animal or a human being, as well as having the ability to program the device remotely is the main motivation for research in the area. For medical applications, this can reduce the invasive procedures that are performed on the body in order to obtain the biological data.

Some of the implantable devices that have been investigated for having an antenna and so the capability of data transmission are glucose sensors, intracranial pressure sensors, ICDs[1] and heart pacemakers. As far as the author is aware, the only commercialized products using antennas are pacemakers and ICDs. These devices are discussed in chapter 2.

In the biological side, the antennas can be used for the purpose of tracking the animals or gathering their biological data in the case of more specific researches. In our study, the goal of the research is to implement an implantable tag which goes under the skin of Steller sea lion. These animals are an endangered species. The tag is supposed to be used as a tracking device as well as a temperature sensor (as a dead or alive signal for population survey purposes).

[1]Implantable Cardioverter Defibrillators

The challenges in the way of implantable antennas are power loss in the biological tissues, the effect of the surroundings on the antenna impedance and antenna efficiency, size constraints and the difficulties of having actual measurements with the live tissues. The biological tissues are extremely lossy and this makes it difficult to get a reasonable level of power out of the body. Another sink for the power is the impedance mismatch between the tissue and the free space. This mismatch results in a significant reflection coefficient and prevents a large portion of power from getting out of the body. If we know the amount of power that we are able to send out of the body, then we can use the other design tools to meet the required qualifications.

Another important aspect of the problem is the impedance change of the antenna inside the tissue. Having a good matching circuit is a necessity in a situation where we have a huge power constraint. In fact this is one of the few controllable factors in transmission. So we should be able to estimate the impedance of the antenna when implanted.

As far as the author is aware, all of the research in the area of implantable devices has focused on the short range applications. That means the goal of the communication link is to send the data outside of the human body to a nearby receiver. Consequently, the reports are more centered on the electronics parts rather than the antenna design. In recent years, the engineers have put more effort in the area of communication link and started to evaluate the implanted antennas more accurately. Numerical and analytical results are dominant in this area. Comparatively, there are less physical experimental measurements performed using the proposed antennas. One of the main reasons is the difficulty of having live tissue measurements. Obviously researchers do not have the right to try the device inside a live human being unless they have the reliable results of the performance. Also in animal related research, there are strict animal care protocols which make tight constraints for the live animal measurements in order to protect animal rights. The fact is that usually engineers are not willing to enter the biological side and deal with the problems of getting the permissions in the area that they are not well familiar with. Therefore many of us prefer to stay in the safe side, for example through using simulations.

Another solution which can be more realistic is the use of simulated tissue phantoms. There are some recipes available for different tissues. Most of them are for the frequency of 403-405 MHz frequency which is the usual frequency for implantable antennas.

In this thesis a loop antenna is proposed for the long range application in the implanted

tag at 915 MHz. In chapter 2 we review the studies on the implanted devices with communication capability. A new method of communication through the biological tissues called volume conduction will be introduced as well. Also a brief explanation of the animal care procedures in Canada is provided, since this is not familiar to most of the engineering community. In the third chapter we will review the analytical results available for the loop antenna and we will also study some specific parameters for our application. The main reasons for choosing the loop antenna are the size constraints of the tag and the fact that the loop has near fields which are dominantly magnetic and so are less affected by the biological tissues. In the last chapter the measurement results of the antenna are presented. The impedance values, frequency shift and the power loss of the antenna when implanted are estimated using a tissue simulating liquid, raw pork meat and also the author's hands.

Chapter 2

Background

The investigations on the implantable antennas can be divided into two categories. One group of studies focuses on implanted devices and designs specific antennas for specific devices. Another group investigates the design and evaluation of the implantable antennas inside the body without referring to any specific application. The following two sections are a literature review of the studies.

The last section reviews the special rules and legislations governing the use of experimental animals in academic projects.

2.1 Implantable Antenna Applications

In this section we will review a number of implantable devices which make use of a communication link to transmit their data. These have been produced specifically for short range applications in which the goal is just sending data outside the human body.

2.1.1 Implantable Cardioverter Defibrillators (ICD)

An implantable defibrillator delivers an electrical shock to terminate fast and chaotic heart rhythms. The device is connected to leads positioned inside the heart or on its surface. These leads are used to deliver electrical shocks, sense the cardiac rhythm and sometimes pace the heart, as needed. The various leads are connected to a pulse generator, which is implanted in a pouch beneath the skin of the chest or abdomen. These generators are typically a little larger than a wallet and have electronics that automatically monitor and

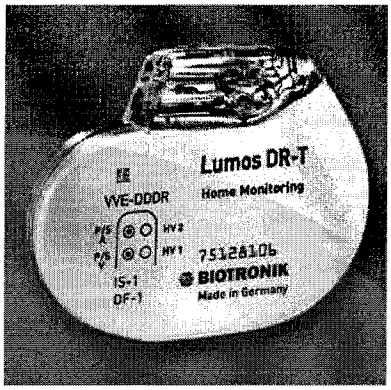

Figure 2.1: Lumos DR-T (the implantable cardioverter defibrillator)(©2004 Biotronik)

treat heart rhythms recognized as abnormal. Newer devices are smaller and have simpler lead systems. They can be installed through blood vessels, eliminating the need for open chest surgery[1].

A patient with an ICD needs to attend regular technical follow up sessions. Technical improvements can theoretically increase the follow-up intervals. However a disadvantage of increased intervals may be the delay in physician's and patient's awareness of changes in clinical status. The follow-up intervals also vary for different patients. Some may need more frequent and more intense follow up sessions due to the medical conditions [Theuns et al, 2003].

The possibility of obtaining the data from the ICD remotely without needing the patient physically be present in the hospital or physicians office is of great interest. The technology of home monitoring for ICDs has been under investigation for more than three decades.

In 1970s, the idea of Trans Telephonic Monitoring (TTM) was introduced to monitor the longevity of the pacemakers [Theuns et al, 2003]. In 1980s the use of TTM was expanded as a diagnostic tool. The clinical utility of TTM was confirmed in 1990 [Gessman et al, 1996]. The disadvantage of this method is that it is dependent on the active cooperation of the patient, as the patient has to place a special device over the implanted pacemaker. In the next generation of home monitoring systems (2001), Lumos DR-T (Biotronik, Berlin, Germany), the ICD transmits the data to a mobile patient device in the form of trend messages and event reports. The data will be transmitted to the Biotronik Service Center.

[1]For more information see the Americal Heart Assosiation website at: http://www.americanheart.org

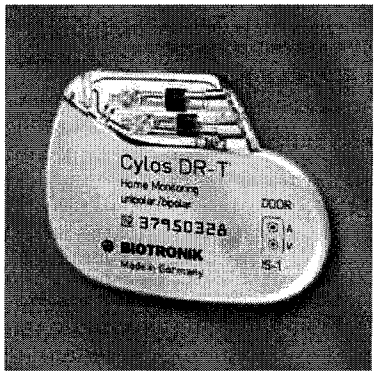

Figure 2.2: Cylos DR-T (the implantable pacemaker)(©2005 Biotronik)

After the data is transmitted via the cellular telephone network, the physician receives a detailed report. The Lumos family is a series of Biotronik products with different abilities. The size of these devices are $55 \times 67 \times 13$ mm and weighs $73gr$. All of them are designed to collect the diagnostic data but only the two latest products, Lumos VR-T and Lumos DR-T have the capability of home monitoring. Transmitter range is about 2 m outside the human body. The reports are sent periodically in fixed intervals. However whenever the ICD detects certain events, a report will be initiated [Biotronik, 2004].

2.1.2 Implantable Pacemaker

Pacemakers are battery-powered implantable devices that are used to electrically stimulate the heart to contract and pump blood throughout the body. Pacemakers consist of a pager-sized housing device which contains a battery, the electronic circuitry and one or two long thin wires that travel through a vein in the chest to the heart. Pacemakers are usually implanted in patients in whom the electrical system of the heart is no longer functioning properly[2]. The only commercialized version of a pacemaker with the data transmission ability is a product of Biotronik Company called Cylos DR-T (Figure 2.2). This device uses the same home monitoring technique that was discussed earlier in ICD section [Biotronik, 2005].

[2]For more information see the Cardiologychannel website at http://www.cardiologychannel.com/pacemaker)

2.1.3 Glucose monitoring telemetry device

The prospective uses for implantable glucose sensors in patients with diabetes include an alarm for low blood-glucose, a continuous read-out of glucose levels and as part of a feedback-controlled insulin delivery system (artificial pancreas) [Pickup, 1993]. Having an implantable glucose monitoring telemetry device can reduce the patient's problems (such as the need to use needles in order to have blood tests) significantly. Atanasov et al (1996) designed a short term glucose sensor which can transmits its data to the outside of the human body. In this design a simple FM radio transmitter is used along with a 5 cm coil antenna. Wikins (1995) proposes a design for a long term sensor. In this device a simple monopole antenna has been used for the data transmission. The difference in longevity of the device is due to the sensing methods.

This device is still under investigation and has not been commercialized yet. Another non-invasive glucose sensing method is based on near-infrared spectroscopy which is also being actively investigated as an alternative strategy.

2.1.4 Implantable Intracranial Pressure Monitor

In some patients with neurological diseases, the intracranial pressure is a vital signal which should be monitored continuously. In the traditional methods to measure intracranial pressure, the physician should make a hole in patient's skull, insert a pressure sensor, and use a wire connected through a bolt in the patient's skull to collect the sensor's data. This method presents reliability and ease of design, calibration and use. However, the transdermal measuring system causes safety hazards. The device is not portable and thus it limits patients' mobility. It also may be a path of infection [Manwaring et al, 2001]. Manwaring et al (2001) introduce an implantable device which is equipped with an intracranial sensor probe and a microelectronic implant. The sensor delivers the information to the microelectronic implant which has a loop antenna for transmission. This device is a passive device which does not have any power supply. An interrogator outside of the patient's body is responsible to get the information from the implant. It is also the power source of the whole system. The interrogator creates an electromagnetic field to establish a communication link with the implanted antenna and also to provide the power for the sensor.

Kawoos et al (2005) introduce a MEMS-based[3] active pressure sensor chip with a 2.4

[3]Micro Electro Mechanical System

GHz Bluetooth chip antenna. The advantages of this device are its long lifetime due to its better biocompatibility and the less chance of infection. The device has a cylindrical volume which is 10 mm in diameter and 8.85 mm in height.

2.2 Antenna Design

Different types of implantable antennas have been designed and investigated numerically, all for short range communication as far as the author is aware. The main challenges in the way of antenna design and data transmission to/from implanted devices are the size constraints of the antenna and the lossy nature of the biological tissues surrounding the antenna. In this section a review on various studies on implantable antennas is presented.

2.2.1 Dipole

The dipole is studied in single [Hurter et al, 1991] and array [Ryan, 1991] forms for hyperthermia applications but there are not many references for the use of dipole for communication in implantable antennas. However Kim et al(2003) have evaluated a half wavelength dipole numerically for implanted devices inside the human skull. The near field and SAR[4] distribution for three different dipole locations were simulated. The pattern of the antenna when placed in different places inside the skull is modeled. It can be seen that when the antenna is placed exactly in the middle of the head (which is an unlikely situation), the internal to the head pattern of the dipole is symmetrical but in the other positions there are distortions in the pattern. The performance of the wireless link between the implanted device and the exterior antenna in terms of the maximum available power at different distances from the head was also evaluated. The antenna is radiating in the $402-405MHz$ frequency band and the transmitted power is 2 μW. The results show that a better than -55 dBm sensitivity is needed at the exterior receiver for a 5m distance form the head.

In another report, [Kim et al, 2004], a dipole antenna is evaluated numerically with two methods of simulation and the results (electric field intensity at different distances form the head) are compared. The methods are spherical Dyadic Green's Function (DGF) expansions and Finite-Difference Time-Domain (FDTD) code. Also the effects of the accuracy of the human body model on the results are studied.

[4]Specific Absorption Rate

2.2.2 Micro Strip Antenna

The first medical application for microstrip antennas has been introduced in [Bahl et al, 1980] for hyperthermia applications [Oh et al, 2005]. In the wireless communication area, microstrip antennas are of interest for implantable applications because of their flexibility in design, conformability and shapes. Also, various methods are available to reduce the size of the antenna such as adding ground pins (thus converting the antenna to a PIFA[5], using relatively huge dielectric constant substrate materials and spiraling the conductor shape (planar helix) [Furse, 2000].

Furse (2000) designed a microstrip antenna and evaluated it numerically for an implantable pacemaker. In [Furse, 2004] a modified microstrip antenna has been evaluated. Furse used a numerical model of human chest using FDTD and calculated the frequency shift of the resonance of the antenna when implanted. The effect of different locations for the feed and the ground point, different materials and thicknesses for substrate and superstrate and different lengths for the antenna have also been studied. Morever two microstrip antennas with the same size and different trace shaped have been compared (Figure 2.3). The size of the antennas are both $26.6mm \times 16.8mm \times 6mm$ and they operate in $402 - 405MHz$ frequency band.

Kim et al (2004) have simulated two spiral microstrip antennas and to PIFAs . The characteristics of the implanted antennas in terms of return loss and radiation efficiency have been evaluated. It is stated that when placed inside the human chest, the radiation efficiency for the microstrip antenna is 0.16% and for the PIFA is 0.25%.

On the other hand in [Johansson, 2004] the patch antennas are considered to be weak antennas when they are placed inside the lossy material and thus for implanted applications. The study shows that the patch inside the tissue does not work well as an antenna.

2.3 Volume Conduction

Other than using RF antennas for transmission of the data through the biological tissue, a method of data transmission has been developed in [Lindsey et al, 1998]. The basic idea of this method is to make use of the ionic and volume conducting properties of the body fluids to transmit data. Using an implanted antenna, a current is injected into the tissue which

[5]Planar Inverted F Antenna

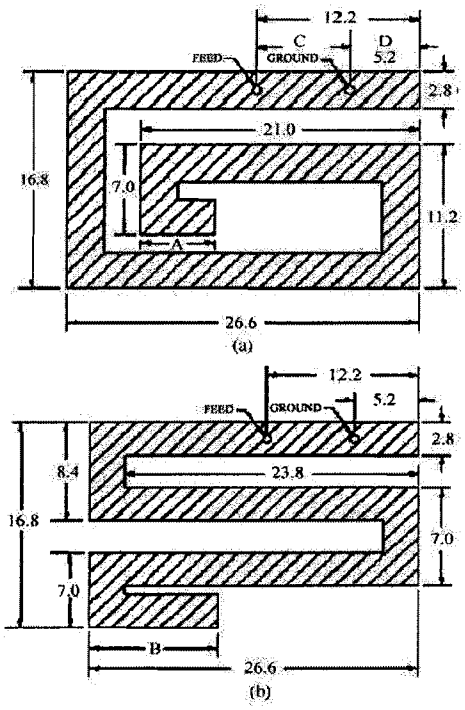

Figure 2.3: The micro strip antennas used in [Furse, 2004](©2004 IEEE)

will produce voltage difference between different locations of the tissue. This voltage will be detected on the surface of the skin using surface electrodes. In this study, the current was injected into a human dead body leg sample using implanted electrodes.

Some of the advantages of this method are as follows [Sun et al, 2003]:

- The lossy nature of the biological tissues is now being used in the transmission process instead of being an obstacle
- The digital to RF data transformation is not needed and thus the power consumption can be reduced significantly
- The communication circuitry is simpler and can be smaller

As the voltage should be measured right on the skin, this method can not be used for long-range data transmission.

Sun et al (2003) have studied the channel properties of a two-way data transmission system using volume conduction method. Sun et al (2003) and Wessel et al (2004) have studied the antenna design for Volume conduction. All of these reports have worked on different designs of x-antenna (figure 2.4) to produce a sinusoidal current with the frequency of 1 KHz . The main goal of the design of the x-antenna is to reduce the amount of shortening current in contrast with the current dipole. The insulator will block the shorting path between the antenna plates. It means that the high current density near the feed of a normal dipole will be reduced. Therefore any potential damages to the surrounding tissues will decrease [Sun et al, 2003]. Furthermore, Sun et al (2005) claim that the far field radiation pattern will improve, but it is not clear what this claim means. Another advantage of the x-antenna is that by making asymmetrical plates, one can change radiation pattern. Depending on the application, there have been different sizes for the antenna, however most of them are around $10mm \times 10mm$.

2.4 Animal Care Protocols

The studies on implantable antennas and devices need to go further than the numerical and analytical results and get some real-world measurements and experimental data. Even the most accurate models can not be perfectly reliable unless they have some accompanying proof of being compatible with the real-world results. Testing implantable devices inside

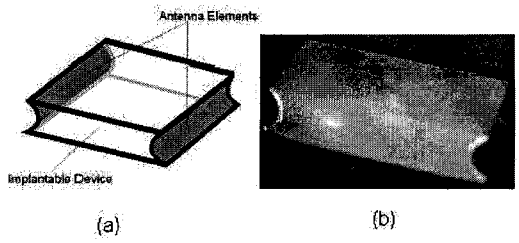

Figure 2.4: The x-antenna design used for volume conduction applications a) Antenna Schematics, b) The actual constructed device. [M. Sun and M. Mickle and W. Liang Q. and Liu and R. J. Sclabassi, "Application of the reciprocity theorem to volume conduction based data communication systems between implantable devices and computers", Proceedings of the 25th Annual International Conference of the IEEE EMBS, September 2003.](©2004 IEEE)

the body of live animals can provide good measurements especially for the research in the field of animal tracking.

When there is a need to use animals as experimental objects, there should also be some rules and regulations to prevent the unnecessary and inhumane use of the live beings. In some countries animal care protocols regulate the use of experimental animals in the process of research. In Canada, the Canadian Council on Animal Care (CCAC) is responsible for this act.

For the work undertaken for this thesis, the author (and also the principal supervisor) were required to gain the Animal Care Certification.

In 1967 the universities and government departments were animals were being used, supported the creation of the Canadian Council on Animal Care. This committee was founded in 1968. The first meeting of the committee was held in January, 1968 and CCAC approved as its goal: "to develop guiding principles for the care of experimental animals in Canada, and to work for their effective application." [CCAC, 1993]

A Resources Panel and an Animal Care Review Panel were established to assist the secretariat in achieving its objective. The functions of the original resources panel have, in recent years, been assumed by specific committees responsible for the development and implementation of national policies on laboratory animal resources.

CCAC assessment panels are responsible for evaluation of the animal care and use in Canadian universities and community colleges, government laboratories, and commercial

laboratories. This program has led to improvement in both housing and management practices. As a result, in spite of the growing research community, the number of experimental animals in use has steadily declined.

The CCAC's Guide to the Care and Use of Experimental Animals requires that institutions conducting animal-based research, teaching or testing set up an animal care committee (ACC) which is functionally active.

2.4.1 Animal Care Committee (ACC)

The animal care committee is responsible to ensure that all of the animal included experiments are compatible with the CCAC legislations. ACC should be responsible directly to senior levels within the institution.

The complement of the committee may vary according to the needs of each institution but it should include the following members [CCAC, 1993]:

- Scientists and/or teachers experienced in animal care and use
- A veterinarian, preferably experienced in experimental animal care and use
- An institutional member whose normal activities do not depend on or involve animal use for research, teaching or testing
- At least one person representing community interests and concerns, and who has no attachment with the institution, and who is not involved in any academic animal experiments
- Technical staff representation (if there are technical staff members actively involved in animal care and/or use within the institution;
- Student representation (in the case of academic institutions)

All research, testing and teaching experiments involving animals should have the ACC approval on their written Animal Use Protocol (discussed below) before being commenced.

As defined in the CCAC Terms of Reference for Animal Care Committees, the ACC has the authority to stop any study that is not being compatible with the approved protocol or where the animals are suffering extreme pain or stress that can not be relieved. In the case of incurable pain or stress, animal may be euthanized. Usually the veterinary staff is given this authority on behalf of the ACC.

Also ACC has the responsibility to inspect all the animal facilities of the institution at least once a year. These inspections insure the compatibility of the animal care facility conditions with the CCAC regulations, identification and resolution of the problems. The report of the inspections are reviewed by the CCAC assessment panels when they visit the institution.

2.4.2 Animal Use Protocol

Before starting any project involving animal use, a written animal use protocol should be handed in to the ACC of the institution to be approved. The protocol should include the following information [CCAC, 1993]

- *Project title*;
- *Project leader(s)*;
- *Principal investigators and other authorized personnel*;
- *Departmental affiliation*;
- *Proposed start date, proposed end date*;
- *Funding agency*;
- *Course number, if a teaching program*;
- *An indication of funding approval*;
- *An indication of the use of biohazardous, infectious, biological or chemical agents*;
- *An indication of biohazard committee approval*;
- *An indication of radioisotope use*;
- *An indication of the categories of invasiveness and the classification of research based on primary use*;
- *Anesthesia and analgesia, including dosages and methods of use*;
- *The method of euthanasia, if necessary*;

- *A description detailing the procedures that are carried out in the animals*;
- *Species and numbers of animals to be used*;
- *Any other information considered important or necessary and pertinent.*

According to [CCAC, 1997], the approved animal use protocol should support the principles of the objective review of animal use in science:

- *The use of animals in research, teaching and testing is acceptable only if it assures to contribute to the understanding of environmental principles or issues; fundamental biological principles; or development of knowledge that can reasonably be expected to benefit humans, animals or the environment*;
- *Optimal standards for animal health and care result in enhanced credibility and reproducibility of experimental results*;
- *Acceptance of animal use in science critically depends on maintaining public confidence in the mechanisms and processes used to ensure necessary, humane and justified animal use*;
- *Animals should be used only if the researcher's best efforts to find an alternative have failed. A continuing sharing of knowledge, review of the literature, and adherence to the Russell-Burch "Three R" tenet of "Replacement, Reduction and Refinement" are also requisites. Those using animals should employ the most humane methods on the smallest number of appropriate animals required to obtain valid information.*

2.4.3 Study on Endangered Species

It seems that there are different levels of sensitivity on different species of experimental animals that can be used through academic experiments. The endangered species can not be used for any kind of experiment. In the case that the research is conducted in the benefit of the species itself, then the researcher should pass some requisite test before starting the experiment with the endangered species. In our study, in order to get to the point where we can implant the tag inside the sea lion body, we were asked to show that the tag would actually work under the animal's skin. Instead of sea lions, the pigs were chosen as the test animals because the skin and fat tissue seemed more likely to resemble the sea lion tissue

characteristics. But still, before starting the test on the pigs, a biocompatibility test needed to be done (on the rabbits) to make sure that the housing of the tag would not have any negative influence on the animal. After this test, again the ACC committee asked for a proof of reliability of the tag in the temperature of the animal body. So the next stage is a test in which the tag will be working for 3 months (the duration of the intended pig test) in the temperature of the animal body. When all of these results are ready and the ACC is convinced that all the predictable problems have been addressed, the pig test will start.

Chapter 3

Loop Antenna

Loops are simple but fundamental forms of antennas. Most of the theoretical results available in the literature deal with the electrically small loop antennas which are of more interest because of their well accepted application in personal communication systems such as pagers and AM radio receivers. The term "small loop" is not exactly defined. Usually a loop with $ka < 0.3$ (where k, the wavelength number, is $2\pi/\lambda$ and a is the radius of the loop) is considered to be small [Balanis, 1983]. However most of the available theoretical results deal with much smaller antennas. In small loops, we can make the assumption of having a constant current around the loop, which makes it relatively easy to analyze. The main characteristic of the loop antenna which makes it interesting as an implantable antenna is the fact that loops have a dominantly magnetic near field and so the important parameter of the surrounding material would be the permeability instead of the permittivity. This could help to decrease the effect of the biological tissues around the antenna. In this chapter some theoretical results on loop antennas are discussed and some different ideas are examined about the best configuration of the loop in an implantable tag. Also the measurement results are compared with the theory about the small and large loops.

3.1 Small Loop Theory

An electrically small loop (circular or square, etc.) is equivalent to an infinitesimal magnetic dipole whose axis is perpendicular to the plane of the loop with the following condition

[Balanis, 1983]

$$I_m l = j\pi a^2 \omega \mu I_0 \tag{3.1}$$

where $I_m l$ is the magnetic moment of the dipole, a is the loop radius and I_0 is the constant current on the loop. As the loop perimeter is assumed to be small compared to the wavelength, the changes in the sinusoidal current can be neglected and the current is considered constant. So, to find the radiation field and other parameters of the loop, one can follow the same procedure as for linear dipoles.

3.1.1 Radiation Field

Figure 3.1 shows the geometry of the circular loop and magnetic dipole. From [Balanis, 1983], the radiation fields of a small loop (infinitesimal magnetic dipole) are

$$H_r = j\frac{ka^2 I_0 cos\theta}{2r^2}\left[1+\frac{1}{jkr}\right]e^{-jkr} \tag{3.2}$$

$$H_\theta = -\frac{(ka)^2 I_0 sin\theta}{4r}\left[1+\frac{1}{jkr}-\frac{1}{(kr)^2}\right]e^{-jkr} \tag{3.3}$$

$$H_\phi = 0 \tag{3.4}$$

where I_0 is the constant current on the loop. It can be seen that only the θ component of the H-field will survive to the far field.

When dealing with a magnetic dipole, we have a magnetic current density instead of an electric one. So we have $M \neq 0$ (magnetic current density) and $J = 0$ (electric current density), and thus the corresponding electric field components are

$$E_r = E_\theta = 0 \tag{3.5}$$

$$E_\phi = \eta\frac{(ka)^2 I_0 sin\theta}{4r}\left[1+\frac{1}{jkr}\right]e^{-jkr} \tag{3.6}$$

where $\eta = \sqrt{\frac{\mu}{\epsilon}}$ is the intrinsic impedance of the medium in which the radiation is taking place.

3.1.2 Power Density

The radiated power for an antenna can be calculated from integrating the power density over a closed sphere. The power density or the poynting vector of an electromagnetic field

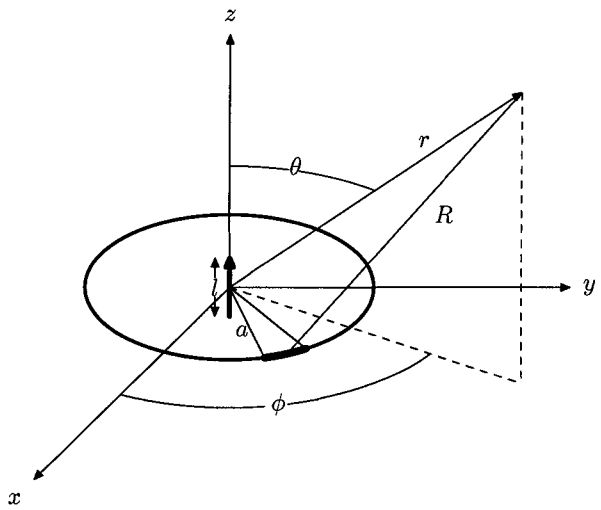

Figure 3.1: The geometery of a circular loop and the equivalent magnetic dipole

is calculated as follows [Balanis, 1983]

$$W = \mathbf{E} \times \mathbf{H} \tag{3.7}$$

where

$$\mathbf{E} = Re\left[E(x,y,z)\ e^{j\omega t}\right] \tag{3.8}$$

$$\mathbf{H} = Re\left[H(x,y,z)\ e^{j\omega t}\right] \tag{3.9}$$

E and **H** represent the instantaneous electric and magnetic field intensities respectively and E and H are the complex envelopes of the fields. So equation (3.7) can be written as

$$\begin{aligned} W &= Re\left[E\,(x,y,z)\ e^{j\omega t}\right] \times Re\left[H\,(x,y,z)\ e^{j\omega t}\right] \\ &= \frac{1}{2}\left[E\ e^{j\omega t} + E^*\ e^{-j\omega t}\right] \times \frac{1}{2}\left[H\ e^{j\omega t} + H^*\ e^{-j\omega t}\right] \\ &= \frac{1}{4}\left[E \times H^* + E^* \times H\right] + \frac{1}{4}\left[E \times H\ e^{2j\omega t} + E^* \times H^*\ e^{-2j\omega t}\right] \\ &= \frac{1}{2}Re\left[E \times H^*\right] + \frac{1}{2}Re\left[E \times H\ e^{2j\omega t}\right] \end{aligned} \tag{3.10}$$

The first term of (3.10) is not a function of time but the second term is time dependent with twice the frequency of the fields. So the time average poynting vector(average power density) will be

$$W_{av} = \frac{1}{2} Re\left[E \times H^*\right] \tag{3.11}$$

The complex poynting vector is defined as

$$W_{av} = \frac{1}{2}\left[E \times H^*\right] \tag{3.12}$$

So the real part of the complex poynting vector is the real radiated power density and the imaginary part presents the reactive stored power density. For the loop antena we have

$$\begin{aligned} W &= \frac{1}{2}(E \times H^*) = \frac{1}{2}\left[(\hat{a}_\phi E_\phi) \times (\hat{a}_r H_r^* + \hat{a}_\theta H_\theta^*)\right] \\ &= \frac{1}{2}(-\hat{a}_r E_\phi H_\theta^* + \hat{a}_\theta E_\phi H_r^*) \\ &= \eta \frac{(ka)^4}{32} |I_0|^2 \frac{sin^2\theta}{r^2} \left[1 + j\frac{1}{(kr)^3}\right] \hat{a_r} - j\frac{\eta k^2 a^3}{16} |I_0|^2 \frac{sin2\theta}{r^2} \left[1 + \frac{1}{(kr)^2}\right] \hat{a_\theta} \quad W.m^{-2} \end{aligned} \tag{3.13}$$

After integrating over a closed sphere with radius r, because of the $\sin 2\theta$ factor in θ component, only the radial component contributes to the complex power P.

$$W_r = \eta \frac{(ka)^4}{32} |I_0|^2 \frac{sin^2\theta}{r^2} \left[1 + j\frac{1}{(kr)^3}\right] \quad W.m^{-2} \tag{3.14}$$

and so

$$P = \oint_S W.ds = \eta \frac{(ka)^4}{32} |I_0|^2 \int_0^{2\pi} \int_0^{\phi} \left[1 + j\frac{1}{(kr)^3}\right] sin^3\theta d\theta d\phi \quad W \tag{3.15}$$

which reduces to

$$P = \eta \left(\frac{\pi}{12}\right) (ka)^4 |I_0|^2 \left[1 + j\frac{1}{(kr)^3}\right] \quad W \tag{3.16}$$

In the far field, the imaginary part of the power is negligible and we just have

$$P_{rad} = \eta \left(\frac{\pi}{12}\right) (ka)^4 |I_0|^2 \quad W \tag{3.17}$$

On the other hand, as can be seen in (3.8), when $kr \ll 1$ the imaginary part is dominant and the power is essentially reactive. The positive sign of the imaginary part of the power shows that the near field power is mainly inductive and the stored magnetic energy is larger than the electric energy.

3.1.3 Radiation Resistance and Ohmic Loss

Using the assumption of having a constant current around a small loop, the radiation resistance of single loop antenna can be found from

$$P_{rad} = \frac{|I_0|^2 R_{rad}}{2} \quad W \tag{3.18}$$

$$\Rightarrow R_{rad} = \eta\left(\frac{\pi}{6}\right)(k^2a^2)^2 = 20\pi^2\left(\frac{C}{\lambda}\right)^4 \quad ohms \tag{3.19}$$

where $C = 2\pi a$ is the circumference of the loop and η is the impedance of the medium which in the case of free space is equal to 120π. If the loop antenna has N turns each being exposed to the same magnetic field, the radiation resistance is

$$R_{rad} = \eta\left(\frac{\pi}{6}\right)(k^2a^2)^2 = 20\pi^2\left(\frac{C}{\lambda}\right)^4 N^2 \quad ohms \tag{3.20}$$

Note that for this equation to hold, the total electrical length of the wire should be small enough to have the constant current still.

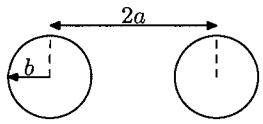

Figure 3.2: Cross section of the single loop

The ohmic losses are calculated directly from the losses in the wire loop. However in a multi turn loop, the spacing between the turns must be greater than five times the wire radius for this assumption to be met. Otherwise, the proximity effect of the turns must be considered which will increase the ohmic loss (the proximity effect will be discussed further in section 3 of this chapter). Considering this proximity effect [Smith, 1972], the total ohmic resistance for an N-turn circular loop is given by

$$R_{ohmic} = \frac{Na}{b}R_s\left(\frac{R_p}{R_0} + 1\right) \quad ohms \tag{3.21}$$

Where

a = loop radius (m)

b = wire radius (m)

$R_s = \sqrt{\frac{\omega\mu_0}{2\sigma}}$ = surface impedance of the conductor (ohms/2)

R_p = ohmic resistance due to proximity effect (ohms)
$R_0 = \frac{NR_s}{2\pi b}$ = ohmic skin effect resistance per unit length (ohms/m)

Here we need the assumption of $\frac{a}{d_s} \gg 1$ where d_s is the skin depth and equal to $\left(\frac{2}{\omega\mu_0\sigma}\right)^{1/2}$. For the case of copper wire, the skin depth is around $2\mu m$ so we can easily assume that the condition is met.

3.1.4 Radiation Intensity and Directivity

The radiation intensity is defined as the radiated power per unit solid angle. This parameter is independent of distance and can be calculated from the power density, i.e.

$$U = r^2 W_{av} \quad W.rad^{-2} \tag{3.22}$$

The average power density, W_{av}, of the antenna has only the radial component W_r from which we calculate the radiation intensity as

$$U = r^2 W_r = \frac{\eta}{2}\left(\frac{k^2 a^2}{4}\right)^2 |I_0|^2 sin^2\theta = \frac{r^2}{2\eta}|E_\phi(r,\theta,\phi)|^2 \quad W.rad^{-2} \tag{3.23}$$

The pattern of the loop is identical to that of the infinitesimal dipole and the maximum value occurs at $\theta = \frac{\pi}{2}$ and is given by

$$U_{max} = U|_{\theta=\pi/2} = \frac{\eta}{2}\left(\frac{k^2 a^2}{4}\right)^2 |I_0|^2 \quad W.rad^{-2} \tag{3.24}$$

The radiation intensity averaged over the sphere is given by

$$U_{av} = \frac{P_{rad}}{4\pi} \quad W.rad^{-2} \tag{3.25}$$

The directivity of an antenna is a parameter which relates only to the radiation pattern. It shows the ratio of the power radiated in a specific direction to the total radiated power. So the directivity of the loop can be found as

$$D_0 = 4\pi \frac{U_{max}}{P_{rad}} = \frac{3}{2} \tag{3.26}$$

3.1.5 Efficiency

The antenna efficiency is defined as $\frac{R_{rad}}{R_{rad}+R_{ohmic}}$. As the radiation resistance of a small loop antenna is so small compared to its ohmic resistance, the antenna efficiency is normally low. However the efficiency can be increased using two different methods

1. Using multi-turns antennas: For loops with N turns, R_{rad} increases in proportion to N^2 while R_{ohmic} increases in proportion to N. So increasing the number of turns will improve the efficiency.

2. Placing a high permeability core made of ferrite material in the wire loop: Using this method, the magnetic flux passing through the loop increases. With ferrite relative permeability $\mu_{rf} = \frac{\mu_f}{\mu_0}$ occupying the core of the loop, the antenna can be analyzed according to the relative effective permeability $\mu_{er} = \frac{\mu_e}{\mu_0}$ and thus the radiation resistance is

$$R_f = 20\pi^2 \left(\frac{c}{\lambda}\right)^2 N^2 \mu_{er}^2 \quad ohms \tag{3.27}$$

The effective permeability has been measured by Wolf (1966) for a cylindrical ferrite core as follows [Vaughan and Anderson, 2003; after Wolf, 1966]:

$$\mu_e = \frac{\mu_f}{1 + D_\mu(\mu_f - 1)} \approx \frac{1}{D_\mu} \quad H.m^{-1} \tag{3.28}$$

where the empirical demagnetization factor is given by $D_\mu \approx e^{-(1.54log(LOD)+0.52)}$ and LOD is the length over diameter of the ferrite core. The formula is held for LODs between about 3 and 100.

3.2 Comparison of the simulation, theory and measurement results of the impedance

As mentioned in the previous section, theoretical analysis for radiation resistance of the loop antenna is available for small loops. In this section we compare the results for the loop resistance and inductance derived from theoretical calculation, simulation and measurement.

We used Wipl-D software to simulate the loop antenna and to find the impedance. For the theoretical calculations we used equation (3.19). In these two cases, the loop is considered to be lossless which means the only resistance is the radiation resistance.

3.2.1 Measurements: Coax Loop

Using a 2-port network analyzer, we measure the impedance of a balanced loop antenna using unbalanced coax cables. One of the solutions is to use off-the-shelf baluns to connect the cable to the load. Another solution is to use a coax cable to make the antenna and the balun at the same time. Figure 3.3 shows the antenna. The inner conductor feeds the antenna at point A. As the loop is symmetrical, B is a neutral point and we do not have any currents coming back into the cable in principle. A simple test can ensure us of the balun working properly. We can move our hands along the cable (lower than point B) and if the measured impedance remains constant, the balun is working properly. We calibrated our measurements (set the reference plane) at point A and thus read the pure impedance of the loop on the test set. Here we have some ohmic losses because of the non-zero losses of the outer conductor of the cable.

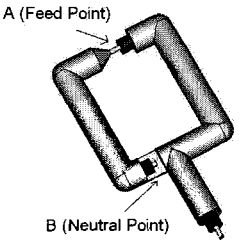

Figure 3.3: The coax cable loop

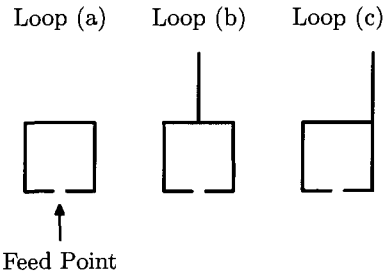

Figure 3.4: Three different configurations of the loop

To check the effect of the part of the cable that is connected to the loop, three different arrangements of a loop antenna have been modeled (Figure 3.4). Figure 3.5 shows the simulation outputs for a square loop with a long wire coming out of one of its corners or sides.

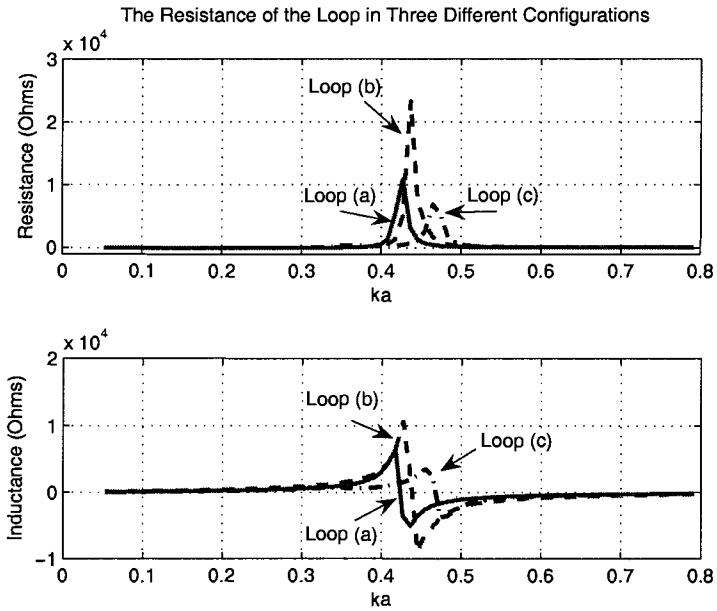

Figure 3.5: The resistance of the different loop configurations given in figure 3.4. The unbalanced configuration makes much more difference to the impedance than the balanced ones.

To have a better perception of the results in lower frequencies, figure 3.6 shows the same results focusing on the region of $ka = 0.1 - 0.3$.

It can be seen that when the schematic is symmetric around the feed point, which results in a balanced structure, the wire does not have a significant effect. On the other hand, when we connect the wire to one of the corners (Figure 3.4: Loop (c)) the anti resonance frequency shifts.

Also the simulation showed that changing the length of the wire which is connected to the loop (when it's in the order of loops perimeter) in the balanced configuration does not have a significant effect on the results. However in the asymmetric schematic, changing the length of the wire will affect the impedance measurements. Figure 3.7 shows this effect

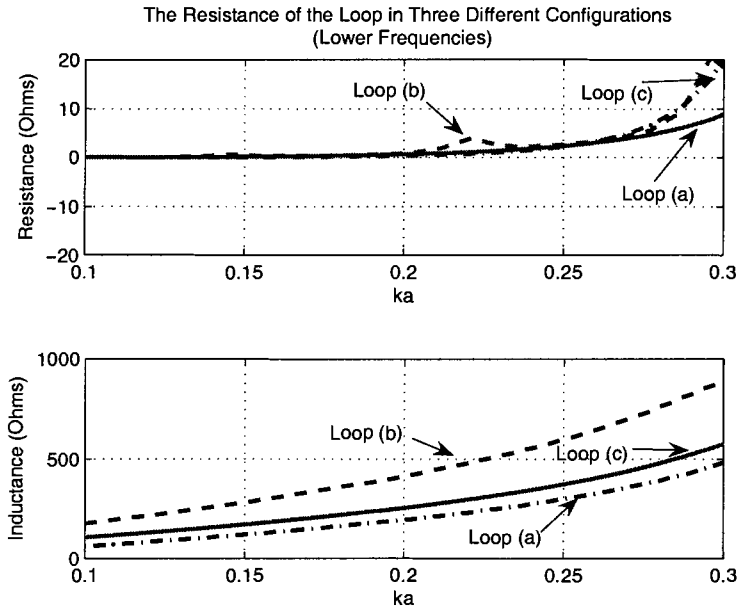

Figure 3.6: The resistance of the different loop configurations in the region of $ka = 0.1 - 0.3$

on the resistance of the loop. The loop perimeter is 10 cm and the frequency range is 30 $MHz - 3\ GHz$.

3.2.2 Results

Figure 3.8 shows the impedance of the antenna. The simulation and theoretical results are well matched for loops with $ka < 0.2$. This can be considered as the largest size that we can consider the loop as small. But the measurement results are moving away from the simulations at $ka = 0.1$. Before this point we have a small difference between the simulation and the measurement which can be a result of having lossless simulations but real measurements. Above the bound $ka = 0.1$ there is a divergence in the results of simulations and that of the measurements. This can be the due to the fact that the simulations are showing the results for a wire loop but the measurements are done with a coax loop. Furthermore, in the experiments the loop is fed by a coax cable but in the simulations we have a balanced voltage feed.

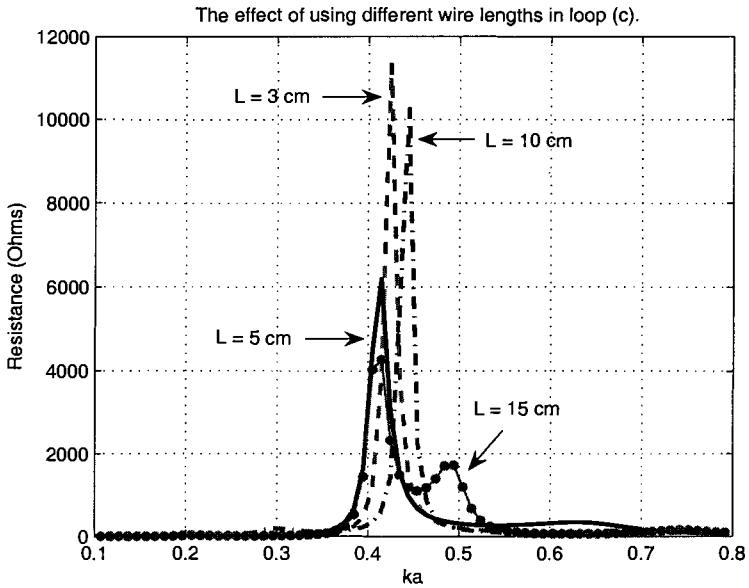

Figure 3.7: The resistance of loop (c) with different lengths of the connected wire. The fequency range is 30 $MHz - 3\ GHz$ and the loop perimeter is 10 cm

3.3 Multiturn loops

One of the main solutions to increase the efficiency through increasing the impedance of the loop antenna is using multi-turn loops. For loops with N turns, R_{rad} increases in proportion to N^2 while R_{ohmic} increases in proportion to N. So increasing the number of turns will improve the efficiency. Usually, R_{ohmic} is directly calculated from the wire losses. However in a multi-turn loop, the spacing between the turns must be greater than five times the wire radius for this assumption to be met [Smith, 1972]. Other wise, the proximity effect of the turns must be considered which will increase the ohmic loss.

3.3.1 Proximity Effect

As mentioned before, considering the proximity effect, the total ohmic resistance for an N-turn circular loop is given by

$$R_{ohmic} = \frac{Na}{b} R_s \left(\frac{R_p}{R_0} + 1 \right) \tag{3.29}$$

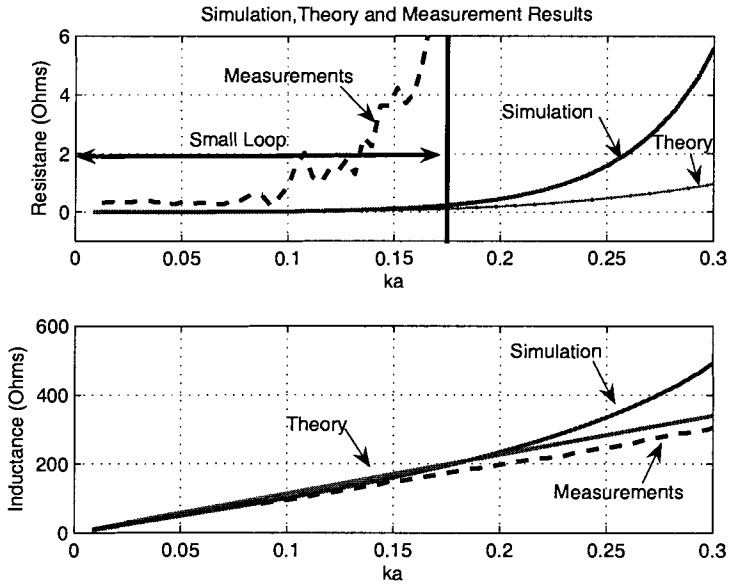

Figure 3.8: The impedance of the antenna: theory, simulation and measurement results.

The fact is that when two current conducting wires are placed next to each other, the current distribution in each of them will be affected by the fields of the other one. This effect will increase the ohmic resistance. Figure 3.9 shows this effect on the surface current of two wires next to each other in comparison to a single wire.

Figure 3.10 shows the cross section of a multiturn loop and 3.11 shows the amount of added resistance due to the proximity effect (Figure 3.10) [Smith, 1972].

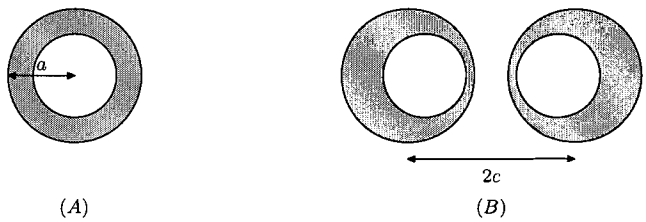

Figure 3.9: The effect of placing two wires next to each other, on their surface current distributions. The thickness of the shadowed area shows the current density

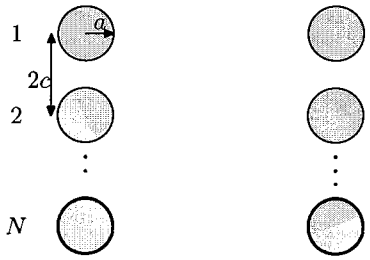

Figure 3.10: N-turn loop ($2c$ is the spacing between the turns).

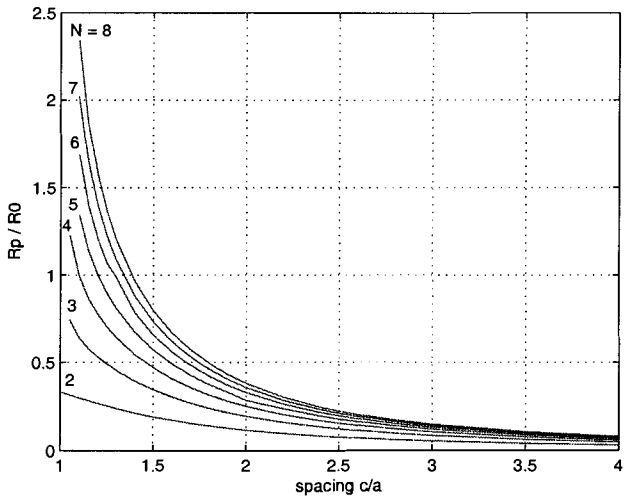

Figure 3.11: Additional ohmic resistance per unit length of a loop having N-turns [Vaughan and Anderson, 2003; after Smith, 1972].

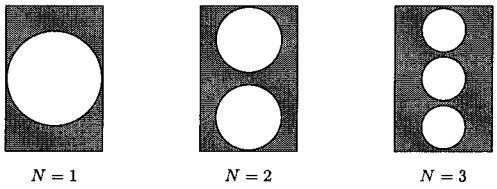

Figure 3.12: The turns cross section. The wire thickness should be reduced, when the number of the turns is increased in a fixed cross section

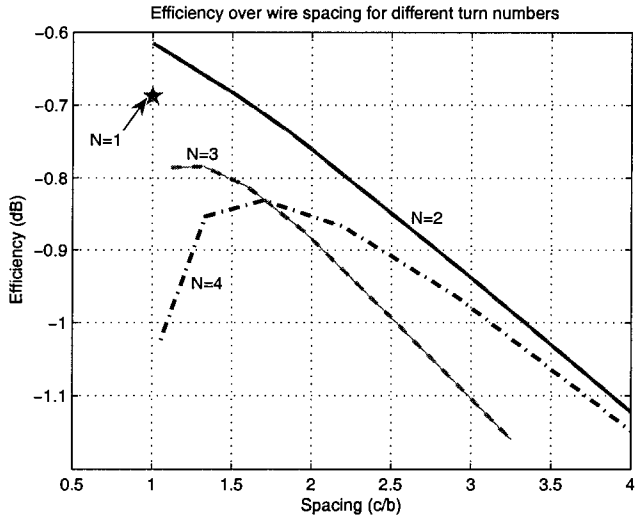

Figure 3.13: The efficiency of multi turn loops in a fixed cross section. It means that we have to decrease the wire thickness in order to get more turns or less spacing (the calculations use Smith's (1972) proximity results).

3.3.2 Space Limitation for Multi-turn Loops

Normally, increasing the number of the turns will increase the efficiency of the loop. However when we have space limitations, in order to increase the number of the turns we have to decrease the thickness of the wire, and consequently the results may change. So we should consider whether the effect of reducing the wire thickness in increasing the ohmic loss is less than the compensated proximity effect.

Figure 3.12 shows how we should reduce the wire thickness if we want to increase the number of turns in a fixed cross section.

Figure 3.13 shows the results of efficiency calculation for different multiturn loops. The

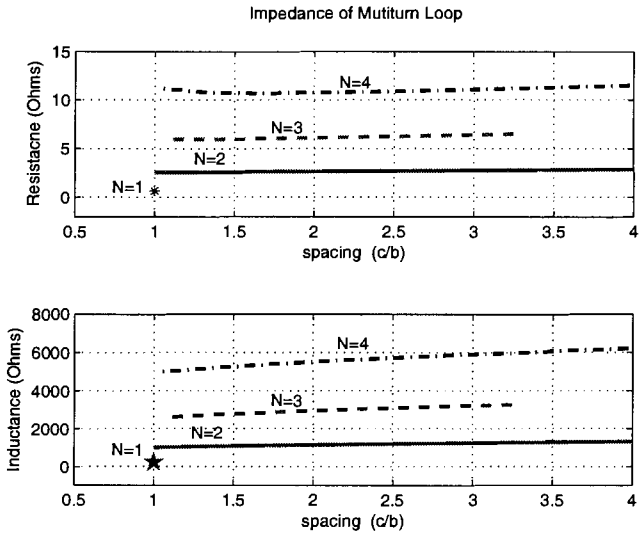

Figure 3.14: The Impedance of multi-turn loops in a fixed space. Both resistance and inductance will increase significantly(the calculations use Smith's (1972) proximity results).

turns are placed in a rectangular space with the maximum area of 2 mm mm and the frequency of the radiation is $915MHz$. $2c$ is the spacing between the turns. Here we have the assumption of constant current for the small loops so the total length of the wire should be less than 0.2 ka to have fairly accurate results. For larger loops the experimental methods or reliable simulations should be used.

It can be seen that the ohmic losses in thinner wires grow so fast that the efficiency drop-off will dominate the effect of using multi turns (except for a small area for 2-turn loops). It means that the cost of decreasing the wire thickness to get more turns with larger spacing is higher than the benefit.

For 3-turn loops and 4-turn loops we have a cross-over in the efficiency. This means that the effect of less proximity and more turns is showing its positive influence on the efficiency but it is not comparable to the efficiency of single loops. There is also an optimum point for the trade-off between the wire spacing and wire thickness for 4-turn loop (i.e. $\frac{c}{b} = 1.7$).

Figure 3.14 shows the resistance and inductance results in the same situation. In some applications, it may be inevitable to loose some efficiency at the cost of mismatch reduction. It means that the impedance change of multi-turn loops may be so favorable that a compromise in efficiency would become acceptable. So, a final decision on the choice of the number

of the turns depends on the specific requirements of the application. When matching losses are of a magnitude that can not be neglected or compensated, the decision should be made between using multiturn loops or having more complicated matching circuits.

Chapter 4

Measurements

It is clear that the medium in which the antenna is radiating influences the performance of the antenna. So, when we insert an antenna into an object, such as the animal skin, the radiation field and the impedance of the antenna will change according to the electrical properties of the tissue and the implementation of the antenna. When we are dealing with transmitting and receiving data from the implantable tags, in order to be able to design a proper matching circuit for the tag, we need to have a good estimation of the impedance variations of the implanted antenna. The problem is that we cannot use the live animals to proceed the first step of the measurements. However, there are different types of tissue simulating liquids which can be used as models for the biological tissues. Measuring the impedance of the antenna in both free space and inside these models, we can investigate the effect of the media on the antenna. We can also use the tissue simulating liquid to estimate the range reduction of the implanted antenna radiation.

4.1 Biological Tissue

When we put the antenna inside the tissue, we are radiating in a high permittivity high conductivity media. The effect of the material on the antenna radiation depends on the dielectric constant or the complex permittivity of the material. Electrically, the dielectric constant can be visualized as a measure of the extent to which a substance concentrates the lines of flux. More specifically, it is the ratio of the amount of electrical energy stored in an insulator to the electric field imposed across it. The imaginary part of the permittivity is

related to the rate at which energy is absorbed by the medium. Here we have

$$\epsilon_r = \epsilon_r' - j\epsilon_r'' \tag{4.1}$$

where

$$\sigma = \epsilon_0 \epsilon_r'' \omega \tag{4.2}$$

In the sea lion project, the tag is to be put under the skin of the sea lion pups. So during the time that the animal grows, the dielectric parameters of the skin will change. The thickness of the skin will increase. Furthermore, the fact that the fur is wet or is dry in the time of transmission will change the transmission properties. The uncontrolled natural parameters in the process are too many that being precise in the modeling of the tissue is not justified (nor likely possible). However, the measurements showed that by having a proper housing for the antenna and the tag, we can significantly isolate the antenna from the outer space parameters. Therefore we used the human skin model as a good estimation of the live sea lion skin.

4.1.1 Biological Tissues Electrical Properties

The real permittivity and the conductivity of some human tissues are shown in table 4.1. Note that the dielectric constants of muscle, skin and blood tissues which have higher water content are much higher than the corresponding values for fat which has lower water content.

Frequency	*Blood*			*Muscle(Skin)*			*Fat*		
(MHz)	ϵ_r'	ϵ_r''	σ	ϵ_r	ϵ_r''	σ	ϵ_r	ϵ_r''	σ
433	62	49.8	1.2	53	59.4	1.43	5.6	3.3	.08
915	60	27.5	1.4	51	31.4	1.60	5.6	1.9	.10
2450	58	15.6	2.1	49	16.2	2.21	5.5	1.1	.16

Table 4.1: The electrical properties of the human tissues in 37° C [Larsen, 1986]

In the sea lion tag project, the antenna is right under the skin at the back of the neck of the animal. Here we do not have any muscle attached to the skin. Moreover the growth of the fat is minimal as the animal grows (Figure 4.1).

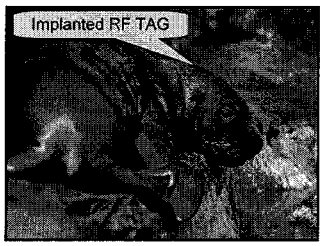

Figure 4.1: Tag spacing inside the animal body

4.1.2 Simulated Tissue

In order to evaluate the implanted antenna performance we make use of tissue simulating liquids. As the transmission line in our project will only include the skin tissues, we can use the muscle (skin) simulating liquids to do our measurements. The following recipe (Table 4.2) is derived from [Johansson, 2004].

Tissue	Water	Sugar	Salt	HEC
Muscle	52.4%	45%	1.4%	1%

Table 4.2: The muscle simulating tissue recipe for $403MHz$ [Johansson, 2004]

Note that HEC is the short term for Hydroxyethylcellolus, which is an inert substance that absorbs the water and increases the viscosity of the solution. This will act to decrease the real part of the permittivity of the liquid.

This recipe is for modeling the muscle in $403MHz$ and its properties are

$$\epsilon_r = 62.5 - 41.5\, j \tag{4.3}$$

$$\sigma = 1 \tag{4.4}$$

However, it can be seen that the difference between the model and the muscle permittivity is more than the variations in the muscle permittivity at higher frequencies. The measurement results show that the same model can be used for higher frequencies as well.

4.2 Impedance and Inductance Measurements

Using the simulating tissue liquid and the coax loop antenna, we performed our measurements in two different conditions. In one case, we directly insert the antenna inside the

material and in the other one we use an ABS[1] housing around the antenna. We also measured the impedance of the antenna putting human hands around it as a loose model for the human muscle. Furthermore as another model for the surroundings, we used raw pork meat.

4.2.1 Measurements Structure

Figure 4.2 shows the antenna, the ABS housing and electronics space in the housing[2]. Also the size of the tag can be compared with the Canadian two dollar coin next to it in the bottom picture. The size and shape of the housing was determined according to the implantation limitations for sea lions.

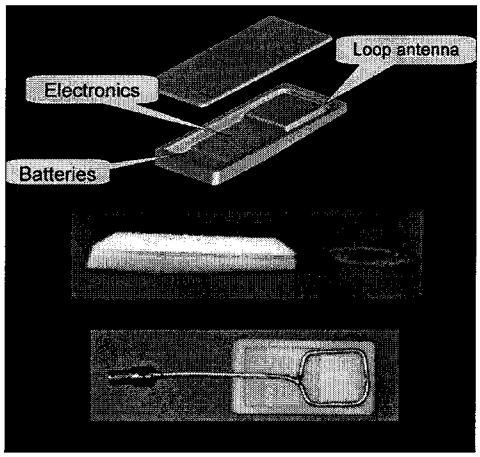

Figure 4.2: ABS housing for the antenna.

Figure 4.3 shows how the measurements inside the tissue simulating liquid were performed. The antenna has been put in the side of the bowl in order to model the tag's proximity and orientation within the animal. The experiments showed that small variations (in the order of millimeters) in the thickness of the liquid did not have a significant effect on the results.

[1] Acrylonitrile Butadiene Styrene, a convenient material for forming prototype shapes

[2] UBC provided the housing

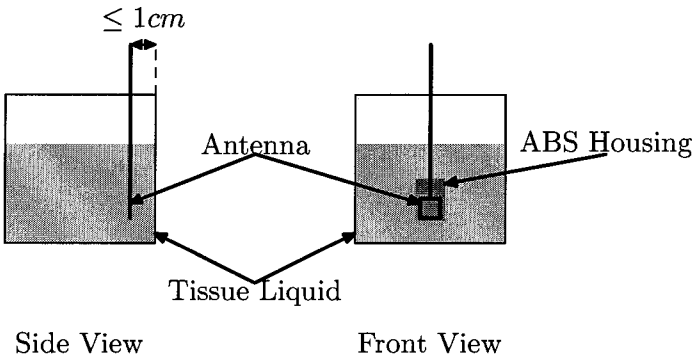

Figure 4.3: Antenna measurement structure in tissue simulating liquid

4.2.2 Variance of the Measurements

All of the measurements are done 5-10 times depending on the variance of the results. In different measurements, the antenna is moved around, in order to eliminate the effect of multipath by averaging over samples. In the cases where the variance of the measurements were relatively higher, we had more samples to get a good estimation of the mean value. Figure 4.4 shows the measurement results for the antenna inside the simulating liquid and the antenna with ABS housing in free space. As it can be seen, the ABS measurements have such a small variance that different measurements are almost indistinguishable. But the measurements in tissue simulating liquid have higher variances.

It will be shown in the following sections that the ABS housing seems to isolate the antenna from the surroundings, and so the small changes do not affect the results. On the other hand, the bare antenna inside the simulating liquid is actually buried in a lossy media and small variations in the thickness of the liquid around the antenna will change the measured impedances.

In order to calculate the estimated standard deviation, we used the following formula [Papoulis and Pillai, 2002]

$$\sigma = \sqrt{\frac{1}{N-1}\Sigma_{i=1}^{N}(x_i - \mu)^2} \tag{4.5}$$

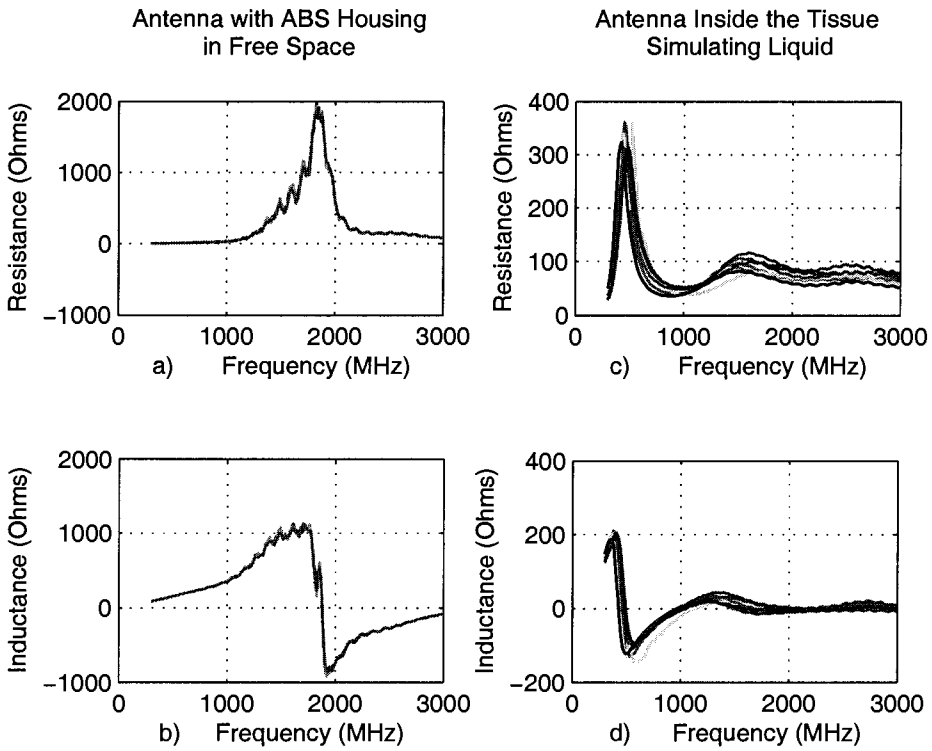

Figure 4.4: Different measurement results for the antenna with ABS housing in free space and the antenna inside the tissue simulating liquid. The free space results are almost indistinguishable between samples but the tissue measurements have a higher variance.

where μ is the estimated mean value of the samples and N is the number of the samples that we have (in our measurements, depending on the variance of the results we have $N = 5$ *to* 10).

Figure 4.5 shows the resistance estimated standard deviation over the estimated mean for all the measurements. On average, the standard deviation of the measurements with the ABS housing is lower than the bare antenna when we put the antenna in a lossy material. The housing reduces the effect of the surrounding on the variation of the measurements. This may be the result of the isolating role of the housing for the antenna. The small changes in the surroundings of the antenna in different measurements have more influence on the results when we have a bare antenna.

In the inductance measurements, the variance is relatively higher because the inductance

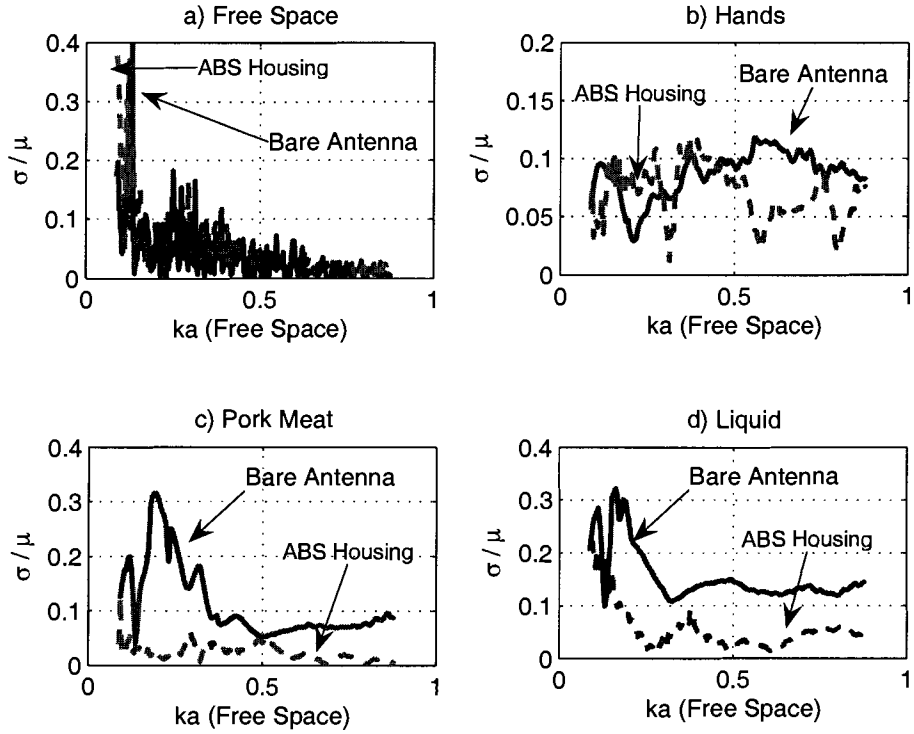

Figure 4.5: Estimated standard deviation of the input resistance measurements a) Bare antenna, b) Antenna with ABS housing)

of the antenna is more sensitive to the surroundings. However, we can still see the great effect of ABS housing in reducing this sensitivity. Figure 4.6 shows the estimated standard deviation over estimated mean for the inductance measurements of the antenna in four different materials. The hikes in the graphs are at the points where we were measuring the zero inductance.

In both resistance and inductance measurements, the variance of the measurements in free space does not have the smoothness of the implanted measurements. This could be a result of the dynamic surroundings and multi path environment in which the experiments are taking place. When the antenna is inside the tissue simulating liquid, the outer space has less impact on the impedance

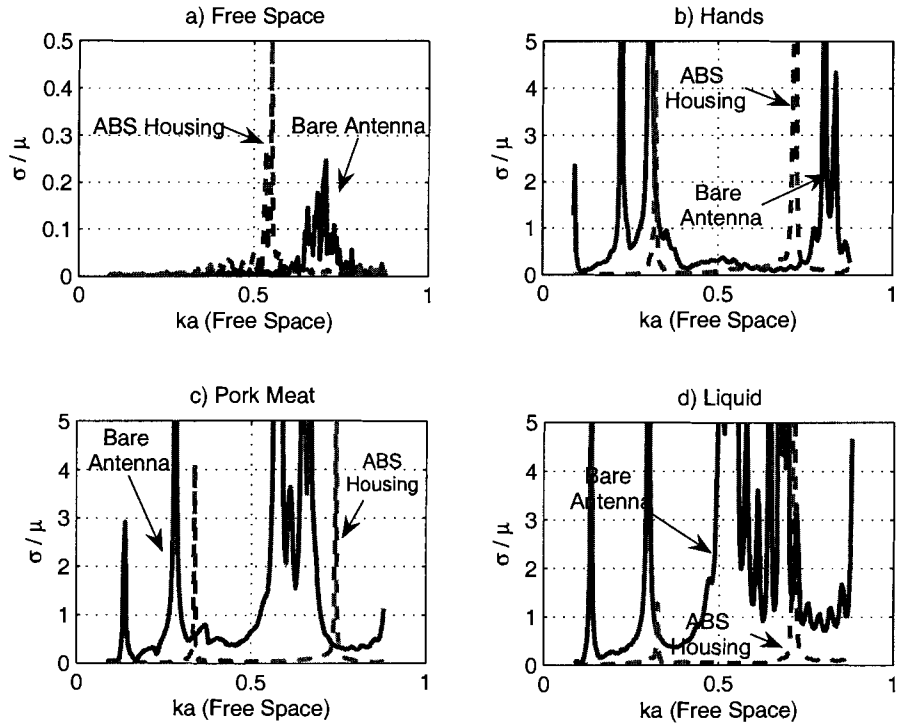

Figure 4.6: Estimated standard deviation of the inductance measurements for four different surroundings a) In Free space, b) Between the hands, c) Inside the pork meat, d) Inside the tissue simulating liquid

4.2.3 Measurement Results: Big Picture

Figure 4.7 shows the effect of the ABS housing on the resistance of the antenna in each of the materials. Graphs (*c*) and (*d*) show that our tissue simulating material is a good model for the muscle tissue (Pork). In the case of bare antenna, we can see that the results from the simulating tissue do not match the results from the antenna inside the hands. This is reasonable because when we put our hands around the antenna, there are many different kinds of tissues (fat, bone, muscle and skin) in the antenna fields. There is also the blood flow which may affect the measurements. However when we use the ABS housing, these three different materials look almost the same (Figure 4.8 shows this more clearly).

Figure 4.9 shows the inductance measurements. Here, we can easily see the anti resonance property of the points where we had hikes in the resistance measurement results. At

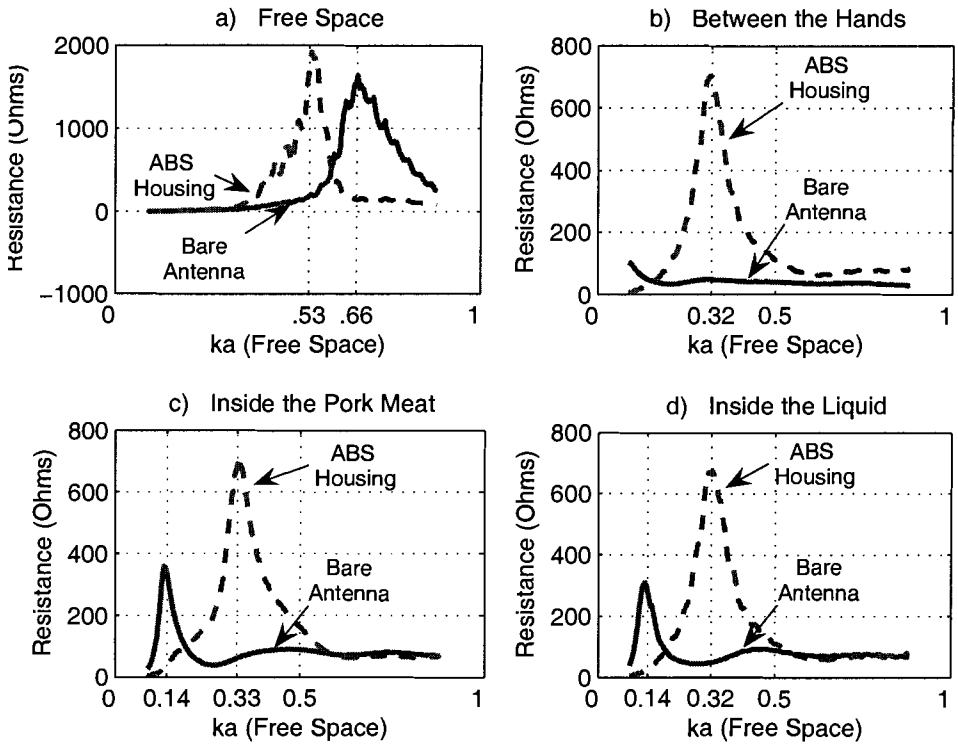

Figure 4.7: Input resistance measurements: a) In Free Space, b) Between the Hands, c) Inside the Pork Meat, d) Inside the Simulating Liquid

these points, we have a huge hike in resistance. The inductance is supposed to go to $+\infty$ and starts to come up again from $-\infty$ theoretically. Also, the effect of the ABS housing can be observed in the same manner as in the resistance results (Figure 4.10).

The frequency shift of the anti resonance point is also decreased in the presence of the ABS housing. As Figure 4.11 shows, for the bare antenna, the anti resonance shifts 1.8 (from 2.25 GHz to 0.45 GHz) when we put the antenna inside the liquid. But for the antenna with ABS housing this shift is reduced to 0.73 GHz (from 1.83 GHz to 1.1 GHz). This result could be predicted because what changes the frequency is the difference between the permittivity of the materials. When an ABS housing ($\epsilon_r \approx 3$) is used, the effective permittivity in free space increases while it decreases in the liquid. So the difference between the permittivity in two situations will be less and we will see a smaller frequency shift.

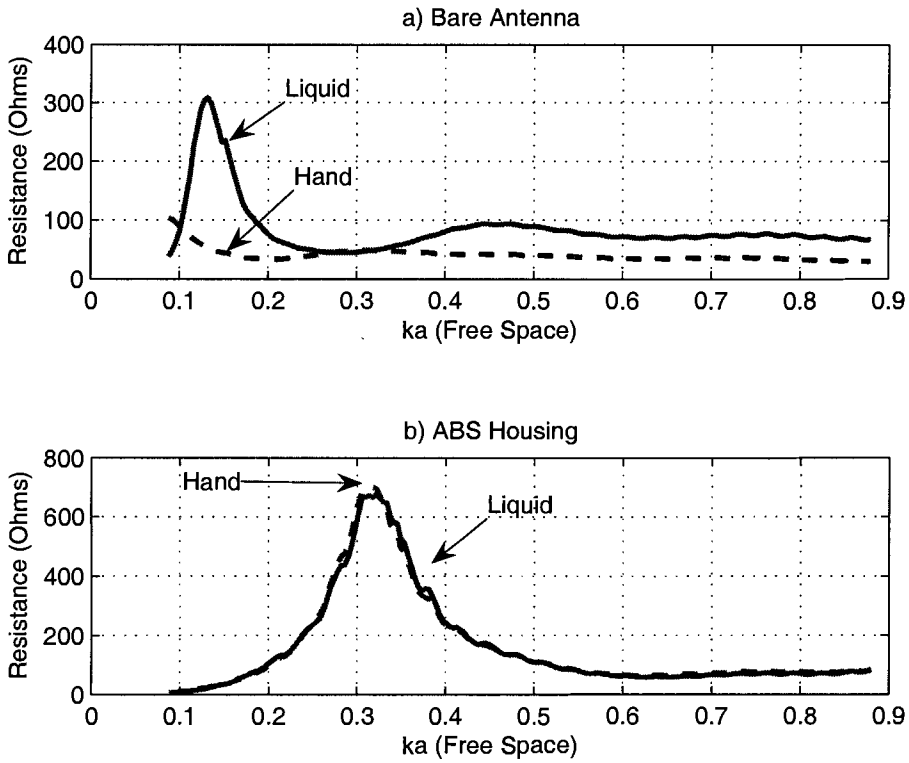

Figure 4.8: The measured input resistance of the antenna between the hands and inside the simulating liquid in the absence and presence of ABS housing. The housing will reduce the resistance difference of the antenna inside the liquid and between the hands.

The measurements of the antenna inside the tissue simulating liquid have been done with the antenna on the side of the liquid bowl, with a distance of about $1cm$ from the free space. The distance is an approximation of the skin tissue thickness for a sea lion implant. However, Figure 4.12 shows that it does not make much difference where to put the antenna. The graph shows the average measurements of the resistance at three different points inside the antenna (form the side to the middle). It can be seen that different lines are indistinguishable.

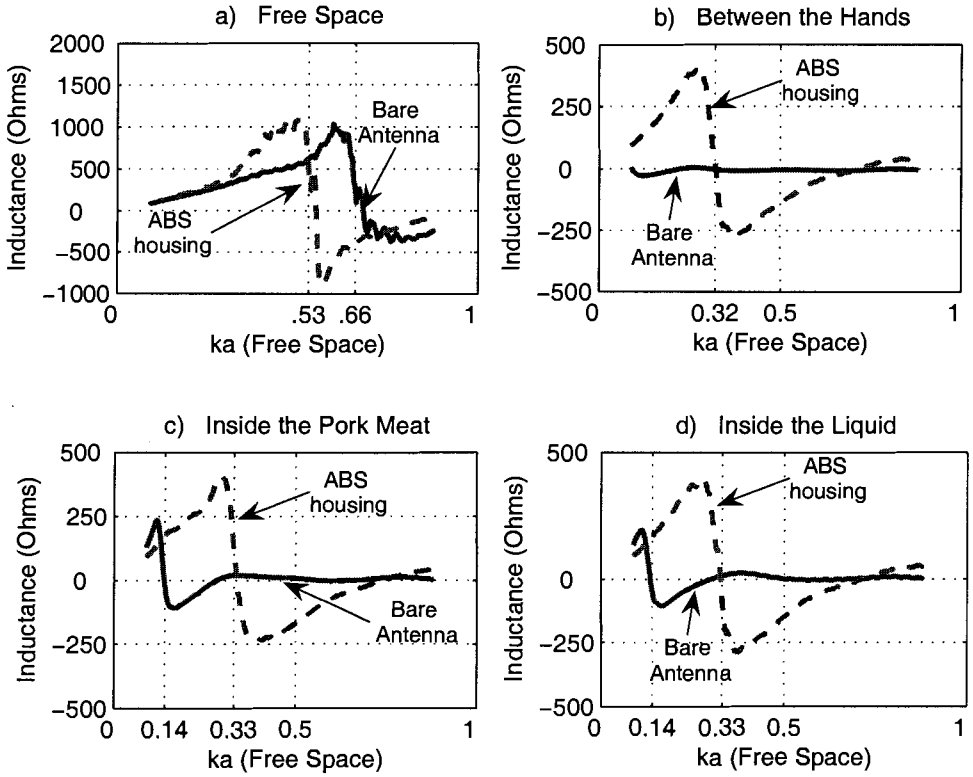

Figure 4.9: Inducatnce measurements: a) In Free Space, b) Between the Hands, c) Inside the Pork Meat, d) Inside the Simulating Liquid

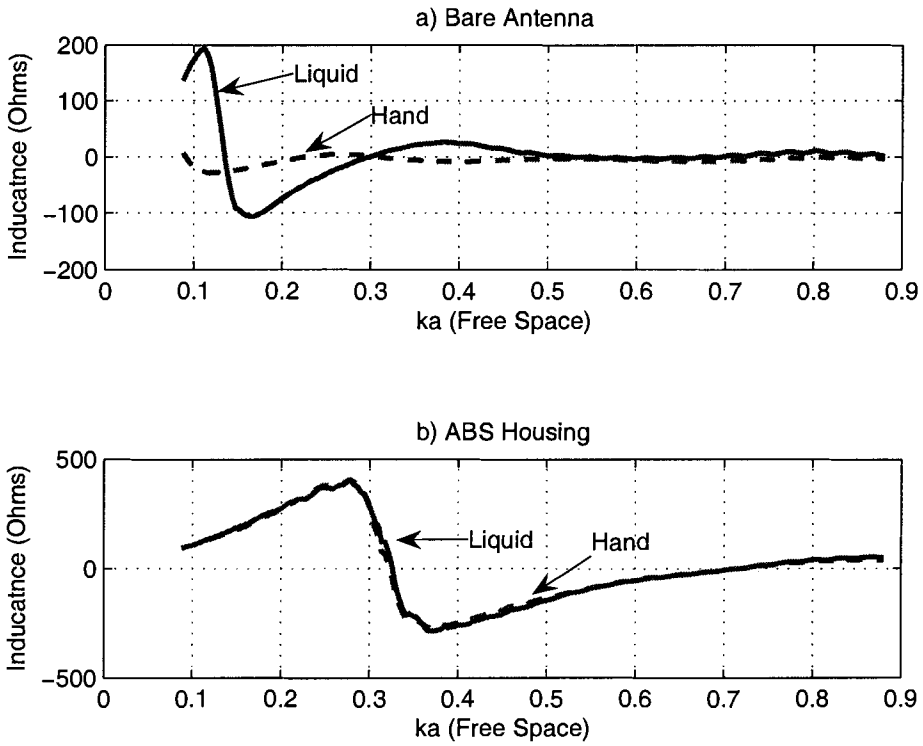

Figure 4.10: The inductance of the antenna: The housing will reduce the inductance difference of the antenna inside the liquid and between the hands.

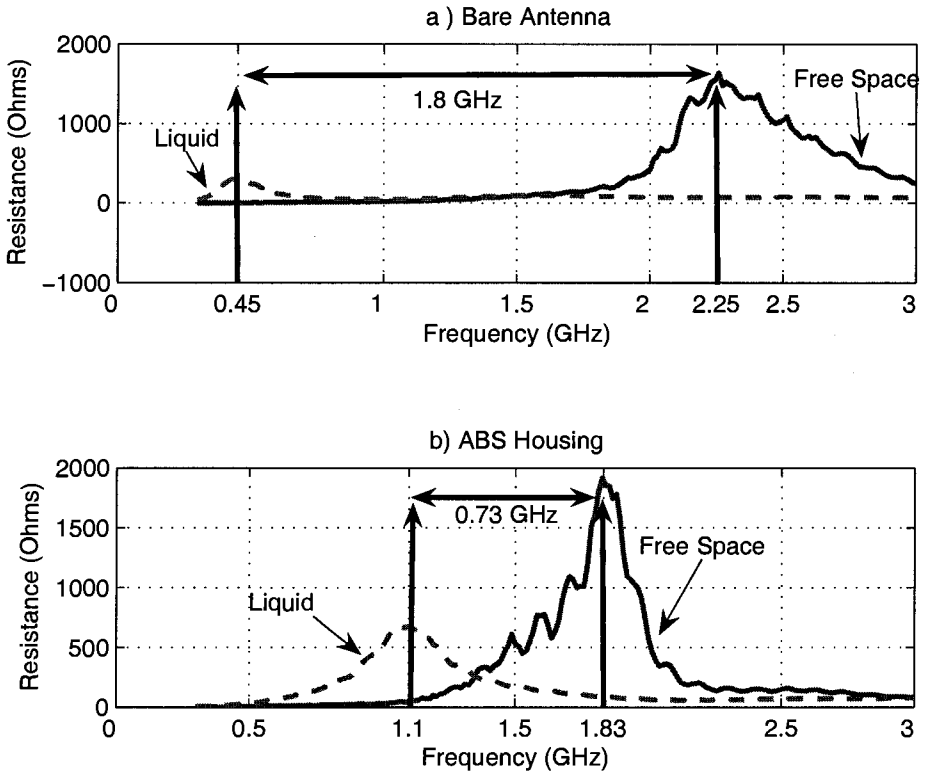

Figure 4.11: The measured frequency shift of the impedance. The ABS housing reduces the frequency shift between the free space and liquid

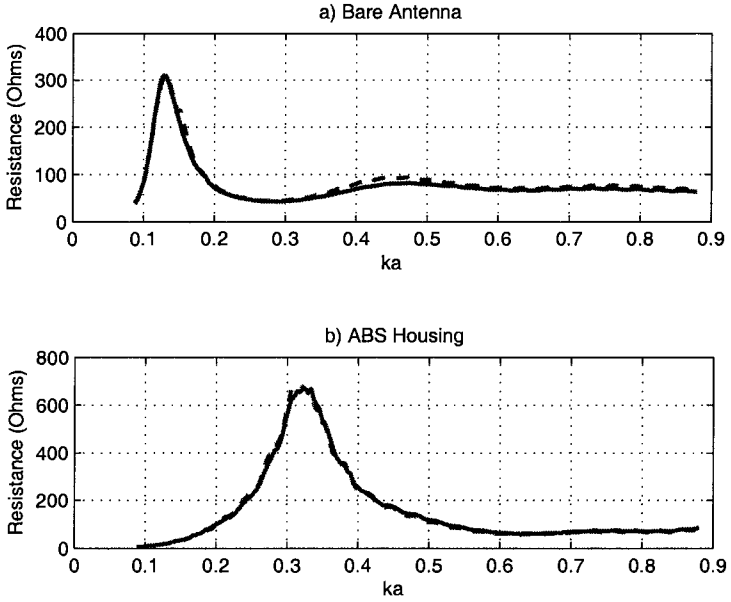

Figure 4.12: Input resistance measurements in different points inside the liquid, a) Bare antenna b) ABS housing. Here, the different graphs are almost impossible to distinguish.

4.2.4 Alumina Housing

The same measurements have been done with alumina housing. Alumina is mechanically stronger than the ABS and so is a better choice for the applications where the implanted tag should bear mechanical pressure. The permittivity of the alumina in 9.15 MHz is about 9. As mentioned before, the difference between the permittivity of the housing and that of the free space will result in a shift in anti resonance frequency. Therefore, when we have a higher change in the permittivity, we expect a larger frequency shift. As the alumina permittivity is three times higher than that of the ABS, the frequency shift is expected to be larger when we use alumina for antenna housing. The reason is that the permittivity of the ABS is closer to that of the free space and it makes a smaller difference than the alumina.

Figure 4.13 shows the results of the measurements in free space and inside the tissues simulating liquid respectively. It can be seen that the alumina housing makes the anti

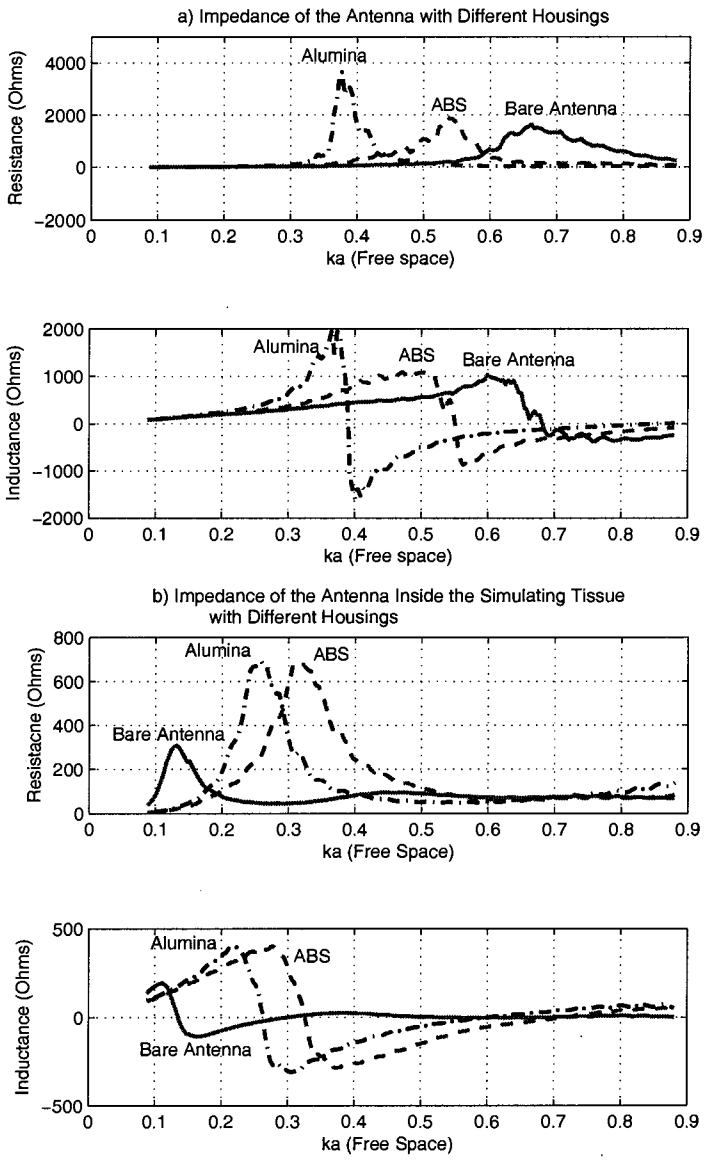

Figure 4.13: The measured impedance of the antenna with different housings a) In free space and b) In tissue simulating liquid.

resonant frequency to shift more. Also we have higher resistances around the central frequency. As expected, because of the higher permittivity of the alumina housing the anti resonance frequency of the antenna with alumina housing is lower in tissue simulating liquid as well (compared to ABS housing). When we put the bare antenna inside the liquid, we are surrounding the antenna with a lossy material. This media acts like a metal around the antenna which will diminish the radiations. Consequently, the frequency properties of the bare antenna are different to the other two graphs. The ABS and alumina are being compared in the same situations and the measurement results show their consistency.

4.2.5 915 MHz

For our design, the 915 MHz frequency has been chosen as a result of previous research on propagation characteristic of the rocky beach areas in which the tags are going to be used. This frequency is chosen from the free frequency bands available from FCC regulations.

At this frequency the electrical size (the perimeter of the loop in wavelengths) of the antenna is $ka = 0.27$. To have a better insight of the impedance in this frequency, we should have a closer look to the measurement results in this range (Fig 4.14). The estimated mean value of the impedance of the antenna with ABS housing inside the liquid is $324+382j$. The estimated standard deviation of the resistance and inductance are 7.1 and 20 respectively. As mentioned before, the imaginary part of the impedance of the antenna is more sensitive to the variations in the surrounding area. On the other hand both measurements are accurate enough when we compare the results with the expected uncontrolled variations in a live animal. The natural factors such as aging, growing and thickening of the fat and skin have much more significant effects on the results than the small variations in the impedance measurements of the model. Therefore, we may not get any benefits from being more precise in the measurements.

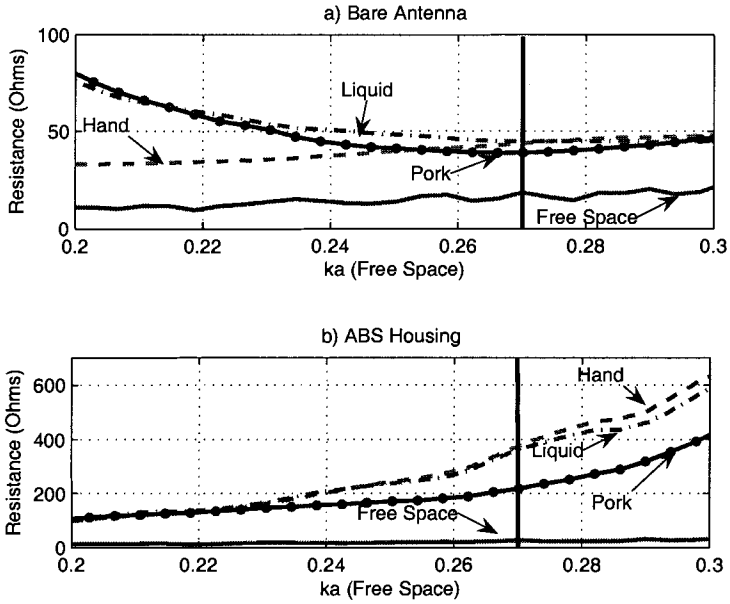

Figure 4.14: The measured input resistance of the a) Bare antenna, b) Antenna with ABS housing (The thick line shows the measurements at 915 MHz).

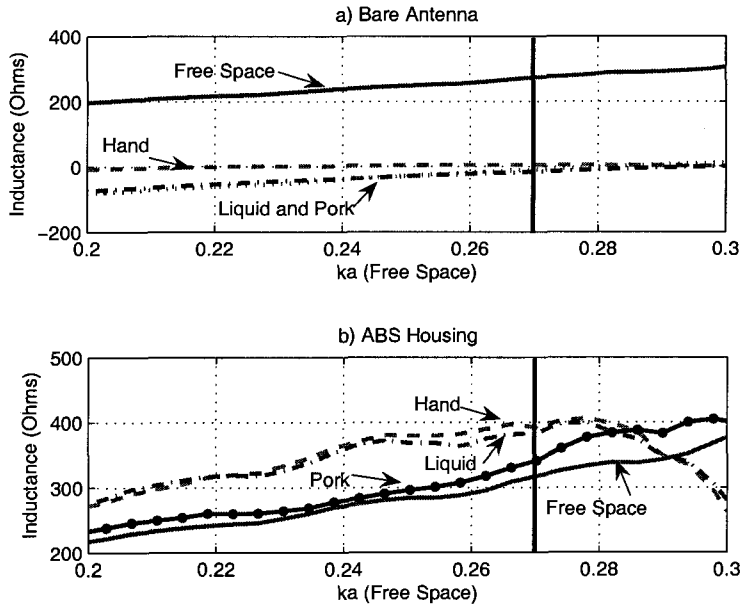

Figure 4.15: The measured inductance of the a) Bare antenna, b) Antenna with ABS housing (The thick line shows the measurements at 915 MHz).

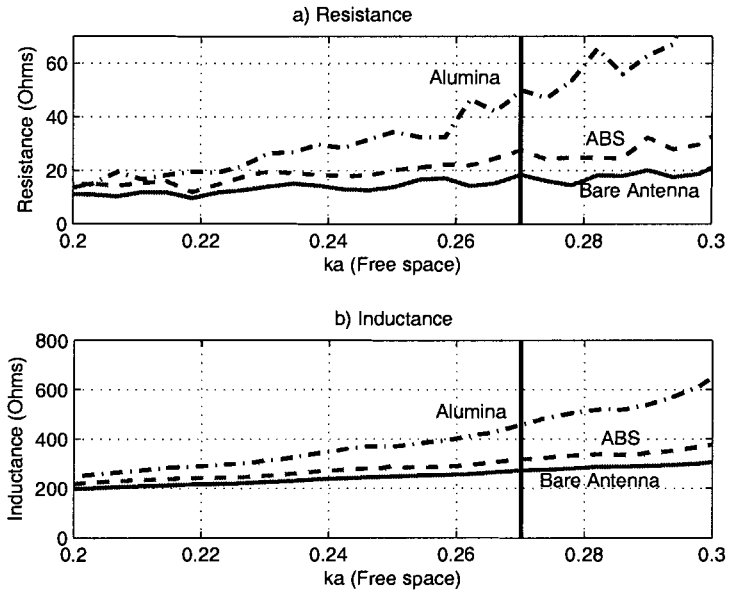

Figure 4.16: The measured impedance of the antenna with different housings in free space around 915 MHz (The thick line shows the measurements at 915 MHz).

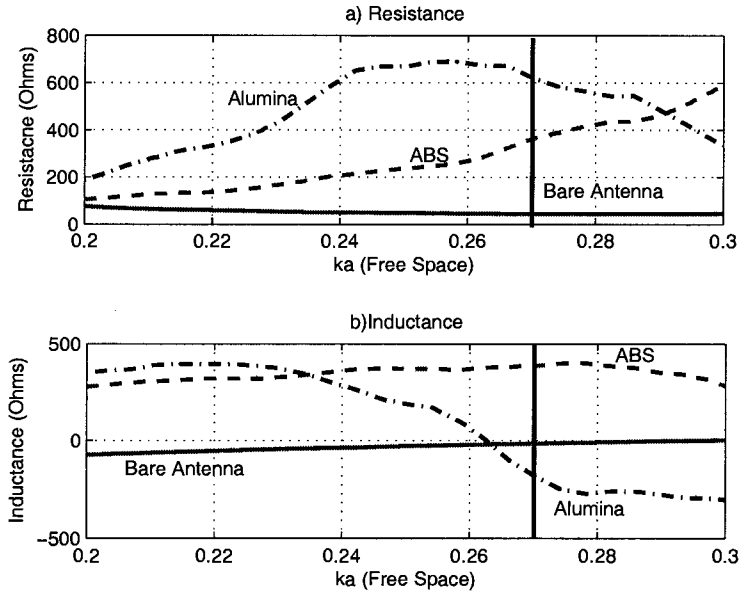

Figure 4.17: The measured impedance of the antenna with different housings inside the tissue simulating liquid (The thick line shows the measurements at 915 MHz)

Figures 4.16 and 4.17 show the resistance and the inductance of the antenna with different housing around the 915 MHz frequency. It can be seen that the most significant change is in the inductance where we have a negative imaginary part for alumina but a positive one for ABS. The reason is that the anti resonance frequency for the antenna with alumina is lower than 915 MHz and in the specified point (915 MHz) we have passed the positive inductance area.

4.3 Frequency Shift: Theory

In theory we have the following formula about the impedance change and frequency shift of an antenna inside a homogenous material with the complex permittivity of ϵ_r [private communication, R.G. Vaughan]

$$Z_{in}(\omega, \epsilon_0) = \sqrt{\epsilon_r}\, Z_{in}(\frac{\omega}{\sqrt{\epsilon_r}}, \epsilon_r) \tag{4.6}$$

In our measurements, we do not see this relationship between the impedance of the antenna in free space and inside the liquid. The reason may be the fact that we are not actually dealing with an infinite media. This means that the near fields are more exposed to the effect of higher permittivity than the far fields. Thus the imaginary part of the impedance is more influenced by a higher effective permittivity than the real part. Also, when we use the ABS or alumina housing, we no longer have homogeneous surroundings and we can not assume to have a constant permittivity around the antenna.

4.4 Power Loss

Another important aspect of the implanted antennas is the power loss. Biological tissues are lossy medias that dissipate significant amount of radiated power. We designed an experiment to compare the antenna's transmitted power in free space and inside the tissue simulating liquid. Figure 4.18 shows how the measurements were performed.

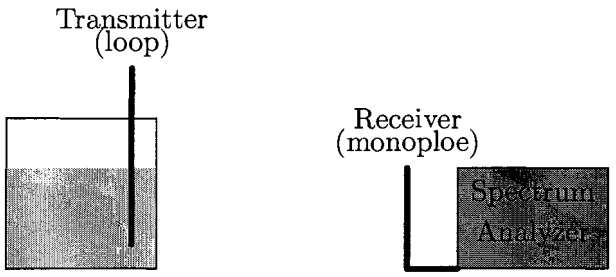

Figure 4.18: Power loss measurement structure

The loop is connected to a transmitter and radiates once in free space and once inside the tissue simulating liquid. The receiver shows the amount of power it receives each time. The difference should be the power loss inside the liquid. But the problem is that the antenna is not matched to the transmitter and we have different reflected powers at the beginning of the transmission. It means that we are actually transmitting different powers and so the received powers can not be compared. To solve this problem we need to consider the reflection coefficients of the transmitter antenna and use the Friis equation to calculate the real transmitted and received power (in the case of polarization matched antennas):

$$\frac{P_{rec}}{P_t} = (1 - |S_{11}|^2)(1 - |S_{22}|^2)G_r G_t G_L \tag{4.7}$$

where P_{rec} is the received power, P_t is the transmitted power, G_r and G_t are the receiver and transmitter gains respectively, G_L is the path gain and S_{11} and S_{22} are the reflection coefficients at transmitter and receiver. Note that we do not consider the polarization mismatch here (assume the polarization efficiency is equal to 1). Also, there is no need to use the receiver's reflection coefficient as it will remain the same in both experiments. The receiver antenna gain will also be the same for both cases. But the transmitter antenna gain may vary putting the antenna in different materials. In our study, due to the unavailability of sufficient equipment to measure the antenna gain, we had to measure the changes in the path gain and the antenna gain together. That means we are unable to separate these two at this point. The test set that we used for our impedance measurements did not have sufficient source power for the power loss experiment. Therefore we used HP 8711C network analyzer which on the other hand, did not have the ability to calculate the reflection coefficients.

Using the Friis equation we see that if we had matched antennas with no reflected power at the transmitter, the received power would have changed at the receiver. We want to compare the power loss of the transmission of the antenna in free space and inside the liquid. So we need to assume that we have matched antennas. In this case, the relation between the measured power with unmatched antenna and the power that we would measure if we had matched antennas is

$$P_{rec-matched} = \frac{P_{rec-unmatched}}{1 - |S_{11}|^2} \tag{4.8}$$

This new parameter can be used in the power comparison between the free space and the liquid.

The reflection coefficients can be calculated from the impedance of the antenna. This experiment has been done in 915MHz where the impedance of the antenna is

$$\begin{aligned} &Free\ Space : 27 + 317j \\ &Inside\ the\ Liquid : 324 + 382j \end{aligned} \tag{4.9}$$

So for S_{11} we have:

$$
\begin{aligned}
& S_{11} = \frac{Zin - 50}{Zin + 50} \\
\Rightarrow \quad & Free\ Space: \ |S_{11}| = 0.97 \rightarrow 1 - |S_{11}|^2 = -13\ dB \\
\Rightarrow \quad & Inside\ the\ Liquid: \ |S_{11}| = 0.88 \rightarrow 1 - |S_{11}|^2 = -6.6\ dB
\end{aligned} \tag{4.10}
$$

The source power in both situations was 23 dBm. At the receiver we used a monopole antenna for this experiment. The received powers are

$$
\begin{aligned}
& Free\ Space: P_{rec} = -31dBm \\
& Liquid: P_{rec} = -29dBm
\end{aligned} \tag{4.11}
$$

The experiments are repeated 3 times and the accuracy of the received power measurement is in the region of $\pm 1.5\ dBm$. According to (4.7) the received power for the case of matched antenna would be

$$
\begin{aligned}
& Free\ Space: P_{rec-matched} = -31dBm + 13dB = -18dBm \\
& Liquid: P_{rec-matched} = -29dBm + 6.6dB = -22.6dBm
\end{aligned} \tag{4.12}
$$

This means we lose 4.6 dB through the tissue simulating liquid. Assuming a situation where the received power is proportional to $\left(\frac{\lambda}{4\pi d}\right)^2$ (line of sight measurements), we can also estimate the change in the range of the antenna. Having $4.6dB$ more power at the receiving antenna (i.e. the same power treshhold for the receiver in both cases) we will have a longer range for the free space. The relation will be

$$
\frac{P_{rec-FS}}{P_{rec-Liq}} = \left(\frac{d_{FS}}{d_{Liq}}\right)^2 = 2.9 \rightarrow \frac{d_{FS}}{d_{Liq}} = 1.7 \tag{4.13}
$$

Where d_{FS} is the range of the antenna in free space and d_{Liq} is the range of the antenna inside the tissue simulating liquid. For example if we measure the range of the antenna to be 500 meters in free space, we will have a 294 meter range for the implanted antenna.

4.5 Matching Slab

The power efficiency of data transmission is one of the main challenges in dealing with implantable antennas. Biological tissues are extremely lossy medias which also feature as reflecting surfaces due to mismatch with outer space. In this section, a matching slab is designed using a simple transmission line model for the transmission of data into the body. This slab will be placed on top of the skin and will perform as a matching device to reduce the amount of reflected power. However, we should add that this method is proper for short range applications.

4.5.1 Transmission Line Model

Figure 4.19 shows a simple model for data transmission through biological tissues. In order to calculate the transmitted and reflected powers, we need to know the characteristic impedance of each layer. This means we need some information about the permittivity and conductivity of different tissues in the way (see Table 4.3) of the incident wave.

Tissue	Muscle(Skin)		Fat	
F(MHz)	ϵ_r	σ	ϵ_r	σ
433	53	1.2	5.6	0.08
915	51	1.6	5.6	0.1
2940	49	2.2	5.5	0.16

Table 4.3: Dielectric Characteristics of biological tissues [Larsen et al, 1986]

For each layer, the characteristic impedance is

$$Z_d = \left(\frac{\mu_0}{\epsilon_o \epsilon_r}\right)^{1/2} \tag{4.14}$$

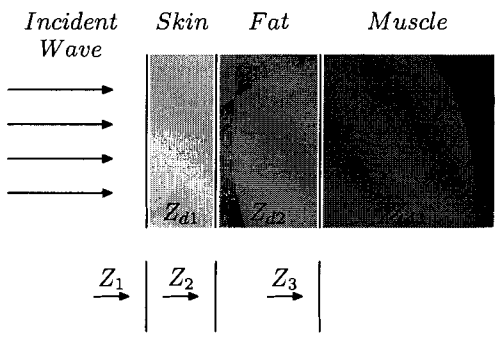

Figure 4.19: Transmission Line Model

For M-layered structures, surface impedances at each layer can be found from the following equations [Anderson, 1986]

$$Z_n = Z_d(n)\frac{Z_{n+1} + Z_{dn}tanh(\gamma_n l_n)}{Z_{dn} + Z_{n+1}tanh(\gamma_n l_n)} \tag{4.15}$$

Here γ is the propagation constant and l_n is the thickness of the n^{th} layer.

Using (4.14) and (4.15) we can find the total reflection and transmission coefficients [Anderson, 1986]

$$\Gamma = \frac{Z_1 - Z_0}{Z_1 + Z_0} \tag{4.16}$$

$$T = \frac{2Z_{dM}}{Z_{dM} + Z_{d(M-1)}} \prod_{i=1}^{M-1} \left(\frac{2Z_{di}}{Z_{di} + Z_{d(i-1)}} e^{-\gamma_i l_i} \right) \times D^{-1} \tag{4.17}$$

where Z_0 is the free space impedance (120π) and the parameter D is

$$D = \prod_{i=1}^{M-1} \left[1 - \left(\frac{Z_{d(i-1)} - Z_{di}}{Z_{d(i-1)} + Z_{di}} \right) \left(\frac{Z_{d(i+1)} - Z_{di}}{Z_{d(i+1)} + Z_{di}} \right) e^{-2\gamma_i l_i} \right] \tag{4.18}$$

In our case, we assume that the antenna is placed right under the skin. That assumption will eliminate the muscle part of the model. Therefore, by transmitted power, we mean the amount of power that enters the fat. The thickness of the skin is assumed to be 5 mm. Note that Γ and T are the voltage coefficients. So the normalized amounts of transmitted and reflected powers are

$$\frac{P_{transmitted}}{P_0} = |T|^2 \tag{4.19}$$

$$\frac{P_{reflected}}{P_0} = |\Gamma|^2 \tag{4.20}$$

Frequency (MHz)	Transmitted power (dB)	Reflected Power (dB)
433	-9.3	-3.4
915	-11.1	-2.1
2940	-11.8	-1.6

Table 4.4: Transmitted and reflected powers for three different frequencies (Skin thickness is 5 mm)

Table 4.4 shows that there is a remarkable power loss in transmissions through the biological tissues. This loss is completely independent from the type of antenna or its efficiency. Therefore it can not be decreased through antenna design techniques. more ever this phenomena will directly affect the range of the antenna and the battery life.

4.5.2 Matching Slab

In order to find the characteristics of the matching slab, we used the following procedure to calculate its impedance and thickness. We model the whole structure as a load and a generator resistance and try to match these two parts (Figure 4.20).

So the slab properties will be as follows

$$Z_{matching} = \sqrt{Z_{Generator} \times real(Z_{Load})} = \sqrt{Z_0 \times real(Z_1)} \tag{4.21}$$

$$L = \frac{\lambda_g}{4} \tag{4.22}$$

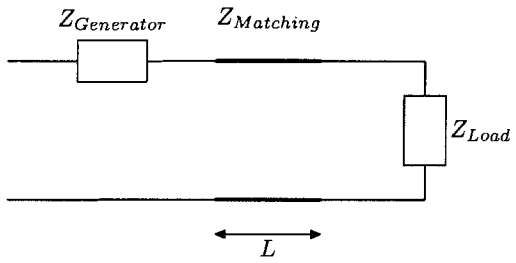

Figure 4.20: The model used for designing the matching slab

where Z_1 is the surface impedance at the skin and λ_g is the guided wavelength which is equal to $\frac{\lambda}{4\sqrt{\epsilon_r}}$. In fact, the complete form of the formula for matching impedance is as follows:

$$Z_{matching} = \sqrt{\frac{real(Z_{Load})|Z_{Generator}|^2 - real(Z_{Generator})|Z_{Load}|^2}{real(Z_{Generator}) - real(Z_{Load})}} \tag{4.23}$$

but because we have a real Z_0 as our $Z_{Generator}$, the formula will be simplified as (4.21). Table 4.5 shows the effect of the matching slab on the amount of transmitted and reflected power. Also the properties of the slab are shown.

Frequency	Transmitted power(dB)		Reflected Power(dB)		Slab Properties	
(MHz)	With Slab	Without Slab	With Slab	Without Slab	ϵ_r	$l\ (m)$
433	-6.7	-9.3	-25	-3.4	5.1	0.08
915	-6.6	-11.1	-14.5	-2.1	8.2	0.03
2940	-5.5	-11.8	-22	-1.6	11.3	0.006

Table 4.5: Transmitted and reflected powers for three different frequencies in the absence and presence of the matching slab

It can be seen that in all the cases, we have a significant improvement in the amount of the transmitted power. Unfortunately, we can not use this method for our tag. The fact that this slab should be placed right outside the body restricts its application to the short

range situations. In long range applications, such as our case where the animal is supposed to live freely in the wild, putting a slab on top of the skin, outside the body, is not a practical solution. However, in many cases the implantable antennas are being used mainly to send the data outside the body. That means that in many of the applications, this slab may be helpful.

Chapter 5

Conclusion

A loop antenna is used for building a communication link with a sub dermal tag which ultimately is to work as a tracking device for Steller sea lions. As a result of size constraints and frequency band limitations, the antenna is not radiating at its resonance frequency. Consequently a matching circuit is needed to reduce the mismatch losses between the transceiver and the antenna. In this thesis, the impedance of the implantable antenna is measured and the effect of the surrounding alterations is studied. It is shown that if we use a lossless high permittivity housing for the antenna we can isolate it from the changes in the surrounding tissues. The results are confirmed using two different types of housing and three different models for animal tissue. We used ABS and alumina housing for the antenna and the measurements were conducted in a tissue simulating liquid which is used to model the human skin, raw pork meat, and live human hands. The results show that the antenna impedance varies when we put the bare antenna inside these materials. However when we use either of the housings, these three surroundings have almost the same effect on the antenna impedance. This study shows that the best antenna is a single turn loop with some low loss dielectric in close proximitty (i.e. housing).

The power loss of the transmission is also studied. Using a known receiver antenna, the power loss of the transmission from inside a tissue simulating liquid is measured and it is known to be around $5dB$ at $915MHz$. Using this result, the range of the antenna is estimated to reduce 1.7 times when it is implanted.

Finally, a matching method is proposed for improving the transmission efficiency especially for short rang applications. In this method a matching slab is placed on top of the skin which will reduce the amount of reflected power at the air and tissue intersection.

This arrangement is not suitable for wild animal testing, but shows the possibility for other applications of energy transmission into or out of lossy matter.

Bibliography

[1] N. Anderson, *The Electromagnetic Field.* New York, Plenum Press, 1986.

[2] P. Atanasov, S. Yang, C. Salehi, A. L. Ghindilis, and E. Wikins, "Short term canine implantation of a glucose monitoring-telemetry device," *Medical Engineering and Physics Journal*, vol. 18, pp. 632–40, December 1996.

[3] I. J. Bahl, S. S. Stuchly, and M. A. Stuchly, "A new microstrip radiator for medical applications," *IEEE Transaction on Microwave Theory and Techniques*, vol. MTT-28, pp. 1464–9, December 1980.

[4] C. A. Balanis, *Antenna Theory, Analysis and Design.* Harper and Row Publishers, New York, 1983.

[5] Biotronik, "Cylos family of implantable pulse generators," *Technical Manual (http : //www.biotronikusa.com)*, 2005.

[6] ——, "Lumos family of implantable cardioverter defibrillators," *Technical Manual (http : //www.biotronikusa.com)*, 2006.

[7] CCAC, "Canadian council on animal care guide to the care and use of experimental animals,vol. 1," *Second Edition (http : //www.ccac.ca)*, 1993.

[8] ——, "Canadian council on animal care guidelines on: Animal use protocol review," *(http : //www.ccac.ca)*, 1997.

[9] C. M. Furse, "Design an antenna for pacemaker communication," *Microwave & RF Journal*, pp. 73–76, march 2000.

[10] L. J. Gessman, R. E. Vielbig, L. E. Waspe, L. Moss, D. Damm, and F. Sundeen, "Accuracy and clinical utility of transtelephonic pacemaker follow-up," *Pacing and Clinical Electrophysiology*, vol. 18, pp. 1032–36, May 1995.

[11] H. Hejase, "Analysis of a printed wire loop," *IEEE Transactions on Microwave Theory and Techniques*, vol. 42, pp. 227–34, February 1994.

[12] W. Hurter, F. Reinbold, and W. J. Lorenz, "A dipole antenna for interstitial microwave hyperthermia," *IEEE Transaction on Microwave Theory and Techniques*, vol. 39, pp. 1048–54, June 1991.

[13] A. J. Johansson, *Wireless communications with medical implants: Antennas and propagation.* PhD thesis, Lund University, Sweden, 2004.

[14] U. Kawoos, M. Mugalodi, M. R. Tofighi, S. Neff, and A. Rosen, "A permanently implantable intracranial pressure monitor," in *Proceedings of the IEEE 31st Annual Northeast Bioengineering Conference*, April 2005, pp. 17–19.

[15] P. Kennedy, "Loop antenna measurements," *IEEE Transactions on Antennas and Propagation*, vol. 4, pp. 610–18, October 1956.

[16] J. Kim and Y. Rahmat-Samii, "An implanted antenna in the spherical human head: Sar and communication link performance," in *Proceedings of IEEE Tropical Conference on Wireless Communication Technology*, October 2003.

[17] ——, "Implanted antennas inside a human body: simulations, design and characterizations," *IEEE Transaction on Microwave Theory and Techniques*, vol. 52, pp. 1934–44, August 2004.

[18] J. D. Kraus, *Antennas*, 2nd ed., ser. McGraw-Hill Series in Electrical Engineering. McGraw-Hill Company, 1973.

[19] L. E. Larsen and J. H. Jacobi, *Medical Applications of Microwave Imaging.* New York: IEEE Press, 1986.

[20] L. Li, M. Leong, P. Looi, and T. Yeo, "Exact solutions of electromagnetic fields in both near and far zones radiated by thin circular-loop antennas: a general representation," *IEEE Transactions on Antennas and Propagation*, vol. 45, pp. 1741–49, December 1997.

[21] D. P. Lindsey, E. L. McKee, M. L. Hull, and S. M. Howell, "A new technique for transmission of signals from implantable transducers," *IEEE Transactions on Biomedical Engineering*, vol. 45, pp. 614–20, May 1998.

[22] M. L. Manwaring, V. D. Malbasa, and K. Manwaring, "Remote monitoring of intracranial pressure," *Annals of the Academy of Studenica*, vol. 4, pp. 77–81, April 2001.

[23] S. Oh and L. Shafai, "Investigation into the cross-polarization of loaded microstrip ring antennas," in *IEEE Antenna and Propagation Society International Symposium*, vol. 1A, July 2005, pp. 243–46.

[24] K. O. Olawale, R. J. Petrell, D. G. Michelson, and A. W. Trites, "The dielectric properties of the cranial skin of five young captive steller sea lions (eumetopias jubatus), and a similar number of young pigs(susscrofa) and sheep (ovis aries) between 0.1 and 10 ghz," *Physiological Measurement*, vol. 26, pp. 625–37, October 2005.

[25] A. Papoulis and S. Pillai, *Probability, Random Variables and Stochastic Processes*, 4th ed. McGraw-Hill Company, 2002.

[26] R. J. Petrell, R. G. Vaughan, R. Virtue, B. Hori, S. Mirabbasi, W. Dunford, A. Trites, and M. Soltanzadeh, "A flat sub-dermal radio frequency identification tag," in *Proceedings of the 16th Biennial Conference on the Biology of Marine Mammals, San Diego, California*, December 2005.

[27] J. Pickup, "Developing glucose sensors for in vivo use," *Trends in Biotechnoloy*, vol. 11, pp. 285–91, July 1993.

[28] T. P. Ryan, "Comparison of six microwave antennas for hyperthermia treatment of cancer: sar results for single antennas and arrays," *International Journal of Radiation Oncology, Biology and Physics*, vol. 21, pp. 403–13, July 1991.

[29] K. Siwiak, *Radiowave Propagation and Antennas for Personal Communications.* Artech House, Boston.London, 1995.

[30] G. S. Smith, "Proximity effect in systems of parallel conductors," *Applied Physics*, vol. 43, no. issue 5, May 1972.

[31] ——, "Radiation efficiency of electrically small multiturn loop antennas," *IEEE Transaction On Antenna and Propagation*, vol. 20, pp. 656–57, September 1972.

[32] P. Soontornpipit, C. M. Furse, and Y. C. Chung, "Design of implantable microstrip antenna for communication with medical implants," *IEEE Transaction on Microwave Theory and Techniques*, vol. 52, pp. 1944–51, August 2004.

[33] B. M. Steinhaus, R. E. Smith, and P. Crosbey, "The role of telecommunications in future implantable device systems," in *Proceedings of 16th IEEE EMBS Conference, Baltimore, MD*, November 1994.

[34] M. Sun, Q. Liu, W. Liang, B. L. Wessel, P. A. Roche, M. Mickle, and R. J. Sclabassi, "Application of the reciprocity theorem to volume conduction based data communication systems between implantable devices and computers," in *Proceedings of the 25th Annual International Conference of the IEEE EMBS*, vol. 4, September 2003, pp. 3352–56.

[35] M. Sun, M. Mickle, W. L. Q., Liu, and R. J. Sclabassi, "Data communication between brain implants and computer," *IEEE Transactions on Neural and Rehabilitation Engineering*, vol. 11, pp. 189–93, June 2003.

[36] M. Sun, B. L. Wessel, W. Liang, P. A. Roche, Q. Liu, M. Mickle, and R. J. Sclabassi, "A volume conduction antenna for implantable devices," in *Proceedings of 25th Annual International Conference of IEEE Engineering in Medicine and Biology Society,*, vol. 4, September 2003, pp. 3356–59.

[37] D. Theuns, J. Res, and L. Jordaens, "Home monitoring in ICD therapy: Future perspectives," *Europace*, vol. 5, pp. 139–42, 2003.

[38] R. G. Vaughan and J. B. Andersen, *Channels, Propagation and Antennas for Mobile Communications.* The Institution of Electrical Engineers, London, UK, 2003.

[39] B. L. Wessel, R. J. Sclabassi, P. Roche, and M. Sun, "Analytical and numerical optimization of and implantable volume conduction antenna," in *Proceedings of the IEEE 30th Annual Northeast Bioengineering Conference*, April 2004, pp. 29–30.

[40] E. Wikins, P. Atanasov, and B. Muggenburg, "Integrated implantable device for long-term glucose monitoring," *Biosensors and Bioelectronics*, vol. 10, pp. 485–94, November 1995.

[41] E. A. Wolff, *Antenna Analysis.* Wiley, 1966.